BACHELOR OF SCIENCE IN ELECTRONIC AND TELECOMMUNICATION ENGINEERING

Performance Evaluation of MIMO in Urban Microcell for Dhaka City at 28 GHz Frequency

Submitted By

MD. Imtiaz Kamrul

T141018

Kazi Mazharul Haque

T141041

Supervised By

Muhammad Mostafa Amir Faisal

Assistant Professor

Department of ETE

International Islamic University Chittagong

Department of Electronic and Telecommunication Engineering
International Islamic University Chittagong
Kumira, Sitakunda, Chittagong – 4314

July, 2018

CERTIFICATE OF APPROVAL

The thesis entitled as "Performance Evaluation of MIMO in Urban Microcell for Dhaka City at 28 GHz Frequency" submitted by **MD. Imtiaz Kamrul** and **Kazi Mazharul Haque**, bearing **ID No: T-141018 & T-141041**, to the Department of Electronic and Telecommunication Engineering (ETE) of International Islamic University Chittagong (IIUC) has been accepted as satisfactory for the partial fulfillment of the requirements for the Degree of B.Sc in Electronics and Telecommunications Engineering and approved as to its style and contents for the examination held on 04th September 2018.

Approved By-

Muhammad Mostafa Amir Faisal
Supervisor
Assistant Professor
Department of Electronics and Telecommunications Engineering
International Islamic University Chittagong

CANDIDATES DECLARATION

It is hereby declared that the work presented in this thesis or any part of this work has not been submitted elsewhere for the award of any degree or diploma, does not contain any unlawful statement.

_____

MD. Imtiaz Kamrul

ID No: T-141018

_____

Kazi Mazharul Haque

ID No: T-141041

ACKNOWLEDGEMENTS

First of all, we would like to convey our gratitude to the Almighty Allah (SWT), for giving us the right direction while attempting the task. It would be inappropriate to call this report complete and successful if we don't thank the people who guided as in the preparation of this thesis. The submission of this project report gives us an opportunity to convey our gratitude to all those who have helped us to reach the stage. We would like to acknowledge the Department of Electronic and Telecommunications Engineering to grant us this opportunity to undertake this thesis. We are very grateful to our supervisor **Muhammad Mostafa Amir Faisal** for the guidance and supervision during the working period of this thesis. Above all, thanks to the great almighty Allah, the author of knowledge and wisdom, for his countless love and for keeping us safe, sound and healthy over the whole period.

ABSTRACT

5^{th} generation cellular network is the upcoming revolution in the cellular communication world. It tends to operate in millimeter wave frequency to increase the usage for the next decade. While the researcher focuses on optimising spectral efficiency and increases bandwidth for incredible demand, only the mmWave spectrum have capability that can accommodate the ever-expanding consumption for the wireless network. The 28 GHz frequency band is a serious candidate for mmWave communication with more than 3 GHz of available bandwidth. The line of Sight (LOS) is a direct line between the radio transmitter and receiver and many types of radio transmissions depend on it. Unfortunately, for arbitrary transmission networks, obstacles are commonly caused by non-line-of-sight (NLOS) conditions. This thesis presents a proper number of selection antenna element in 28 GHz frequency in NLOS and LOS environment and their characteristics by analysis of different channel parameter in Urban microcell scenario for Dhaka city. This thesis also discusses the radio propagation mechanisms that impact the performance of the network in the form of time delays, received power, azimuth AoD, Elevation AoD, Azimuth AoA, Elevation AoA, path-lost and RMS delay in LOS and NLOS environments.

Contents

List of Figures

List of Tables

List of Symbols

Hz	-	Hertz
KHz	-	Kilo Hertz
MHz	-	Mega Hertz
GHz	-	Giga Hertz
mm	-	Millimeter
cm	-	Centimeter
m	-	meter

List of Abbreviations

PDP	-	Power Delay Profile
mmWave	-	Millimeter Wave
AoA	-	Angle of Arrival
AoD	-	Angle of Departure
PLE	-	Path Loss Exponent
HPBW	-	Half Power Beam Width
UMi	-	Urban Micro Cell
UMa	-	Urban Macro Cell
RMa	-	Rural Macro Cell
D2D	-	Device to Device
V2V	-	Vehicle to Vehicle
LOS	-	Line of Sight
NLOS	-	Non Line of Sight
MIMO	-	Multiple Input Multiple Output
NIST	-	National Institute for Standards and Technologies
OTA	-	Over the Air
MPC	-	Multipath Component
TDD	-	Time Division Duplex
CSI	-	Channel State Information
IoT	-	Internet of Things
ULA	-	Uniform Linear Array
URA	-	Uniform Rectangular Array

CHAPTER 1

Introduction

1.1 Introduction

The rapidly increasing demands from consumers for high data rates, ubiquitous connectivity, high-quality video streaming, and low-latency control or communication are driving the development of fifth-generation (5G) wireless communications [1, 2]. Compared to 4G/International Mobile Telecommunications-Advanced (IMT-Advanced) standards, 5G is envisioned to support a higher density of mobile broadband users, better implementation of Internet of Things (IoT), virtual reality, augmented reality, and many other use cases. There is currently no standard for 5G deployments, but the millimeter-wave (mmWave) spectrum (from around 30 gigahertz (GHz) to 300 GHz) is expected to be a key ingredient due to its massive amount of raw available bandwidths [2]. In July 2016, the Federal Communications Commission (FCC) in the United States approved nearly 11 GHz of spectrum above 24 GHz for 5G, including the 28 GHz, 37 GHz, 39 GHz, and 64 - 71 GHz bands [3], which was more than four times larger than the total amount of licensed spectrum currently available for mobile services.

1.2 Technologies Required to Realize 5G

The demand for cellular data traffic continues to outstrip forecasts and is currently growing at a rate of 40-70% per annum [4, 5]. This growth rate implies that relative to current levels, a 1000 times capacity increase within the next decade may be required to be met by the new radio capabilities of the fifth-generation (5G) wireless communications [1, 2, 6, 7, 8, 9, 10, 11, 12]. The capacity gains required by 5G are expected to be provided by:

- Massive multiple-input multiple-output (MIMO) antenna arrays at base stations (BSs) and smaller arrays at the mobile user equipment (UE) [13, 14, 15, 16, 17, 18, 19]

- Increased spectrum bandwidth and use of wideband (> 100 MHz) channels [20, 21]
- Multi-user and three-dimensional (3D) MIMO [22, 23, 24, 25, 26]

1.3 Importance of Selection Proper Channel Parameter in 5G Systems

The radio channel is fundamental to wireless communications [27]. Almost every aspect of wireless communications, ranging from real-world performance prediction, equipment design and system design, antenna architectures, and system performance, to capacity and coverage evaluation, depends upon an accurate understanding of the performance of radio signals when they propagate via a radio channel. The modeling of a radio channel is therefore vital to wireless communications research [28, 29, 30].

1.4 NYUSIM 5G Channel Simulator

1.4.1 Overview

NYU WIRELESS conducted mmWave measurements from 2012 through 2017, having acquired a total of over 1 Terabytes of data, at frequencies from 28 to 73 GHz in various outdoor environments in UMi, UMa, and RMa environments. The measurements and analysis done in [2, 30, 31, 32, 33, 34, 35, 36, 37, 38, 39, 40, 41] led to this NYUSIM channel simulator.

NYUSIM performs drop-based Monte Carlo simulation to generate a CIR at each drop (i.e., user location) assuming no user mobility. Channels for different user locations are assumed to be independent, justified by small correlation distances (up to about 10 centimeters) found in measurements [42]. NYUSIM provides an accurate rendering of actual CIRs in both time and space, as well as realistic signal levels that were measured, and may be utilized to support realistic physical layer and link layer simulations such as those conducted in [30, 43, 44, 45]. The models and simulation approach in NYUSIM involves the research of more than a dozen graduate and undergraduate students, and as of

late 2017, over 10,000 downloads of NYUSIM have been recorded. NYUSIM is applicable for a wide range of carrier frequencies from 500 MHz to 100 GHz, and RF bandwidths from 0 (continuous wave (CW)) to 800 MHz.

It is worth noting that in the 3GPP TR 38.901 Release 14 channel model for frequencies above 6 GHz [46], the number of clusters is unrealistically large. For example, in the UMi street canyon scenario, the number of clusters in the LOS environment is as high as 12, and 19 in the NLOS environment, which is not supported by the real-world measurements at mmWave bands [2, 34, 35, 38]. In contrast, in the SSCM implemented in NYUSIM [82], the number of time clusters ranges from 1 to 6, and the mean number of spatial lobes is about 2 and is upper bounded by 5, which are obtained from field observations and are much smaller than those in the 3GPP channel model [30, 33, 46, 41]. The impractical number of clusters in the 3GPP channel model is likely to result in a higher rank of mmWave channels, unrealistic eigen-channel distributions, and thereby inaccurate spectral efficiency prediction for 5G mmWave channels [30, 41].

1.4.2 Channel Model Implemented in NYUSIM

The broadband SSCM [34] developed by NYU WIRELESS is used in NYUSIM with some important extensions such as including MIMO antenna arrays, adding atmospheric attenuation into path loss, adding more propagation scenarios, generating directional PDPs using accurate directional antenna patterns, etc., to extend the SSCM to the NYUSIM channel model and a standalone channel simulation software [33]. The SSCM is introduced in [34].

1.4.3 MIMO Antenna Arrays at Both TX and RX

In NYUSIM, antenna arrays, such as uniform linear arrays (ULAs) and uniform rectangular arrays (URAs), are allowed to be equipped at both the BS and UE. The entries in the MIMO channel matrix H are obtained by extending the omnidirectional CIR over the antenna array manifold at the TX and/or RX.

1.4.4 Range Extension

Extensive mmWave propagation measurements conducted by NYU WIRELESS have shown that in dense urban environments, mmWave signals can cover around 200 m cell radius even under NLOS conditions [2, 35, 47], and is likely to reach 500 m in lightly populated urban and suburban areas. Furthermore, recent RMa propagation measurements at 73 GHz demonstrated over 10 km coverage range in clear weather [36]. To make NYUSIM cater for more users and wider applications, the maximum allowable T-R separation distance is extended from 500 m to 1 km in NYUSIM v1.6, by removing all the lower bounds on received power (including cluster power, sub path power, and lobe power), or equivalently, upper bounds on path loss, assuming there exits such a virtual receiver that can detect very low received power.

For LOS environments, calculated path loss beyond 500 m is still accurate using the NYUSIM path loss models since they are applicable to over 10 km distances. For NLOS environments, however, the NLOS path loss models employed in NYUSIM may not be accurate for distances larger than 500 m since they were developed for ranges within 500 m [48], thus caution should be given when setting the distance beyond 500 m for UMi or UMa NLOS scenarios. The dynamic range for multipath components in the extended range is extended to 220 dB from the default value of 190 dB used for distances no larger than 500 m.

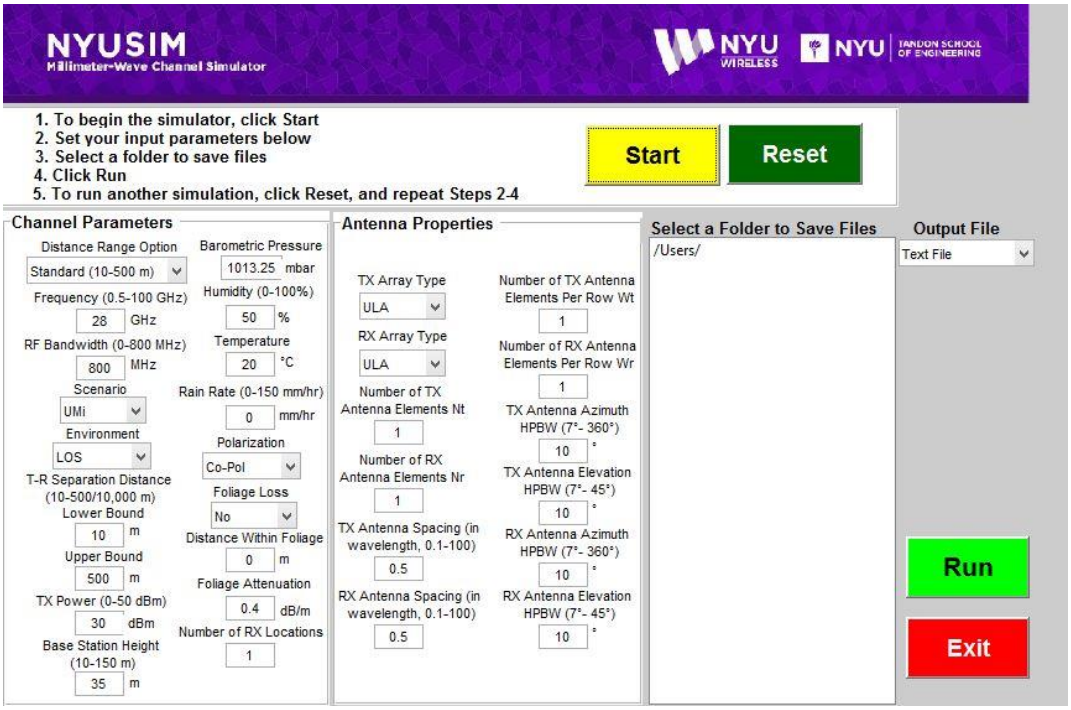

Fig. 1.4.4.1. Graphical User Interface of NYUSIM

1.4.5 Input Parameters

There are 30 input parameters to the channel simulator, which are grouped into two main categories: Channel Parameters and Antenna Properties, as shown on the GUI in Fig. 1.4.4.1 The panel Channel Parameters contains 18 fundamental input parameters about the propagation channel, as listed and explained below:

1. **Distance Range Option:** A selectable parameter denoting the distance range. Two options, “Standard (10-500 m)”, and “Extended (10-10,000 m)”, are applicable. The default setting is “Standard (10-500 m)”.

2. **Frequency (GHz):** An editable parameter denoting the carrier frequency in GHz. The default value is 28 (GHz), and it can be varied from 0.5 to 100 (GHz) with at most one decimal point.

3. **RF Bandwidth (MHz):** An editable parameter denoting the RF bandwidth of the transmitted signal in MHz. The default value is 800 MHz, and it can be varied from 0 to 800 MHz. As the simulator was developed from real-world measurements obtained with an RF bandwidth of 800 MHz, it can only scale down from 800 MHz.

4. **Scenario:** A selectable parameter denoting the scenario. Three options, "UMi", "UMa", and "RMa", are applicable.

5. **Environment:** A selectable parameter denoting the environment, either LOS or NLOS. The default setting is LOS.

6. **Lower Bound of T-R Separation Distance (m):** An editable parameter denoting the smallest distance between the TX and RX in meters with at most one decimal place.

7. **Upper Bound of T-R Separation Distance (m):** An editable parameter denoting the largest distance between the TX and RX in meters with at most one decimal place.

8. **TX Power (dBm):** An editable parameter denoting the transmit power in dBm. The default value is 30 (dBm), and can be set to any value ranging from 0 to 50 (dBm).

9. **Base Station Height (m):** An editable parameter denoting the base station height in m. The default value is 35 (m) [46], and can be set to any value ranging from 10 to 150 (m) [36]. This base station height is only applicable to RMa modeling and is ignored for other scenarios.

10. **Barometric Pressure:** An editable parameter denoting the barometric pressure in mbar used in evaluating propagation path loss induced by dry air. The default and typical value is 1013.25 mbar (millibar) (i.e., nominal for sea level), and may range from 10−5 to 1013.25 (mbar) [49].

11. **Humidity:** An editable parameter denoting the relative humidity in percentage used in evaluating propagation path loss induced by vapor. The default value is 50 (%), and can be set to any number between 0 and 100 (%).

12. **Temperature:** An editable parameter denoting the temperature in degrees Celsius used in evaluating propagation path loss induced by haze/fog. The default and typical value is 20 (°C), and may range from -100 to 50 (°C) [49].

13. **Rain Rate:** An editable parameter denoting the rain rate in mm/hr. used in evaluating propagation path loss induced by rain. The default value is 0 (mm/hr.), and the typical range is 0 to 150 (mm/hr.)

14. **Polarization:** A selectable parameter denoting the polarization relation between the TX and RX antennas or antenna arrays. The default setting is Co-Pol (co-polarization), and can be changed to X-Pol (cross-polarization). The cross-polarization discrimination (XPD) can vary from 5 dB to 27 dB [50, 51, 52], depending on the frequency and environment. In this simulator, for Co-Pol, no extra loss will be added to the path loss, while an extra 25 dB loss will be added to the path loss for X-Pol due to polarization mismatch based on the measurement results in [52]. For more detailed background, please refer to [52].

15. **Foliage Loss:** A selectable parameter indicating whether or not foliage loss will be considered in the simulation. The default setting is No (which implies foliage loss will not be considered), and can be changed to Yes (which means foliage loss will be considered).

16. **Distance Within Foliage:** An editable parameter representing the distance in meters that the transmitted signal travels within foliage. The default value is 0, and can be set to any non-negative number no larger than the lower bound of the T-R separation distance.

17. **Foliage Attenuation:** An editable parameter denoting the propagation loss induced by foliage in dB/m. The default value is 0.4 (dB/m) based on the measurement results in [53],

and can be set to any value between 0 and 10 (dB/m). For more detailed background, please refer to [52].

18. **Number of RX Locations:** An editable parameter denoting the number of RX locations. It can be any positive integer number. The default value is 1, and can be set to any integer from 1 to 10,000.

- The panel Antenna Properties contains 12 input parameters related to the TX and RX antenna arrays, as listed and explained below:

1. **TX Array Type:** A selectable parameter denoting the TX antenna array type. The default setting is ULA, and can be changed to URA.

2. **RX Array Type:** A selectable parameter denoting the RX antenna array type. The default setting is ULA, and can be changed to URA.

3. **Number of TX Antenna Elements Nt:** An editable parameter denoting the total number of TX antenna elements in the array. The default value is 1, and can be set to any integer from 1 to 128.

4. **Number of RX Antenna Elements Nr:** An editable parameter denoting the total number of RX antenna elements in the array. The default value is 1, and can be set to any integer from 1 to 64.

5. **TX Antenna Spacing (in wavelength):** An editable parameter denoting the spacing between adjacent TX antennas in the array in terms of the carrier wavelength. The default value is 0.5, and can be set to any positive number with up to one decimal place from 0.1 to 100. Note that larger antenna spacing leads to lower spatial correlation hence higher achievable rate [45]. Also, no antenna mutual coupling considered for simplicity, likely to

result in more optimistic achievable rate for closely-spaced (e.g., less than 0.5 wavelength spacing) antennas [14].

6. **RX Antenna Spacing (in wavelength):** An editable parameter denoting the spacing between adjacent RX antennas in the array in terms of the carrier wavelength. The default value is 0.5, and can be set to any positive number with up to one decimal place from 0.1 to 100.

7. **Number of TX Antenna Elements Per Row Wt:** An editable parameter denoting the number of TX antennas in one dimension when the TX Array Type is ULA or URA, which should divide the number of TX antenna elements. The default value is 1.

8. **Number of RX Antenna Elements Per Row Wr:** An editable parameter denoting the number of RX antennas in one dimension when the RX Array Type is ULA or URA, which should divide the number of RX antenna elements. The default value is 1.

9. **TX Antenna Azimuth HPBW (degrees):** An editable parameter denoting the azimuth HPBW of the TX antenna (array) in degrees. The default value is 10°, and can be set to any value from 7° to 360° (since the smallest azimuth HPBW of the antennas used in the measurements for the simulator was 7°).

10. **TX Antenna Elevation HPBW (degrees):** An editable parameter denoting the elevation HPBW of the TX antenna (array) in degrees. The default value is 10°, and can be set to any value from 7° to 45° (since the smallest elevation HPBW of the antennas used in the measurements for the simulator was 7°).

11. **RX Antenna Azimuth HPBW (degrees):** An editable parameter denoting the azimuth HPBW of the RX antenna (array) in degrees. The default value is 10°, and can be set to any value from 7° to 360°.

12. **RX Antenna Elevation HPBW (degrees):** An editable parameter denoting the elevation HPBW of the RX antenna (array) in degrees. The default value is 10°, and can be set to any value from 7° to 45°.

The antenna pattern employed in [34] has the following form:

$$G(\phi,\theta) = \max\left(G_0 e^{-\alpha\phi^2-\beta\theta^2}, \frac{G_0}{100}\right), \text{Where} \alpha = \frac{4\ln(2)}{\emptyset_{3dB}^2}, \beta = \frac{4\ln(2)}{\theta_{3dB}^2}, G_0 = \frac{41253\eta}{\phi_{3dB}\theta_{3dB}} \quad (1.4.5.1)$$

where (ϕ, θ) denote the azimuth and elevation angle offsets from the boresight direction in degrees, G_0 is the maximum directive gain (boresight gain) in linear units, $(\phi_{3dB}, \theta_{3dB})$ represent the azimuth and elevation HPBWs in degrees, (α, β) are parameters that depend on the HPBW values, and $\eta = 0.7$ is a typical average antenna efficiency.

The radiation pattern of a sectored cell site antenna was employed in [54], where the azimuthal radiation pattern is modeled as a cardioid given by [54]

$$r(\theta) = \alpha[1 + \sin(\theta + \frac{\pi}{2})] \quad (1.4.5.2)$$

where r is the gain of the antenna at azimuth angle θ from its maximum lobe and is a scaling factor. The elevation radiation pattern is an ellipse with the base station at a focus point [108]:

$$\frac{x^2}{a^2} + \frac{y^2}{b^2} = 1 \quad (1.4.5.3)$$

A sectored antenna pattern model was introduced in [55], where constant directivity gains are assumed for the main lobe and the side.

1.4.6 Output Data Files

For each simulation run, five sets of .txt files and five corresponding mat files are generated, namely,

“AODLobePowerSpectrumnLobex.txt”,

“AODLobePowerSpectrumn.mat”,

“AOALobePowerSpectrumnLobex.txt”,

“AOALobePowerSpectrumn.mat”,

“OmniPDPn.txt”,

“OmniPDPn.mat”,

“DirectionalPDPn.txt”,

“DirectionalPDPn.mat”,

“SmallScalePDPn.txt”,

and “SmallScalePDPn.mat”, where n denotes the nth RX location (i.e., nth simulation run), and x represents the xth spatial lobe. After N continuous simulation runs with the same input parameters are complete, another three .txt files and three corresponding. mat files are produced, i.e.,” BasicParameters.txt”,” Basic- Parameters.mat”,” OmniPDPInfo.txt”, ”OmniPDPInfo.mat”, ”DirPDPInfo.txt”, and ”DirPDPInfo.mat”. Each text file “AODLobePowerSpectrumnLobex” is associated with the output figure of 3D AoD power

spectrum, and contains five parameters (columns) of each resolvable multipath component in an AoD spatial lobe. Figure 1.4.2 and 1.4.3 shows sample 3-D AoA and AoD power spectrum respectively and figure 1.4.4 and 1.4.5 shows the sample omnidirectional and directional power delay profile respectively.

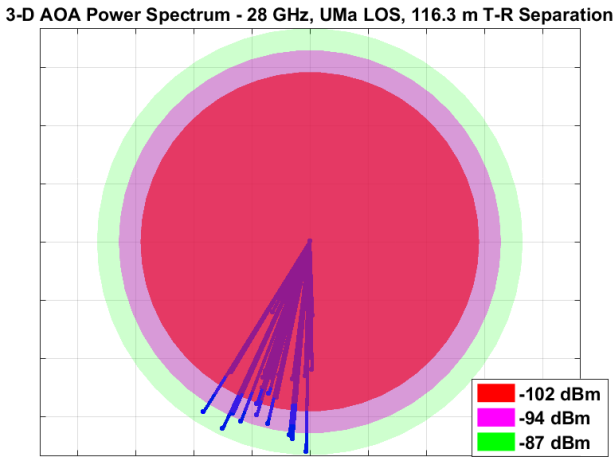

Fig. 1.4.6..1. Sample AOA Power Spectrum generated from NYUSIM. Top view of azimuth plane.

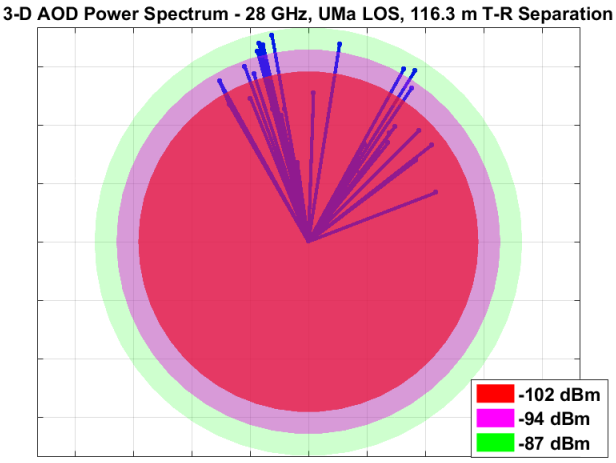

Fig. 1.4.6..2. Sample AOD Power Spectrum generated from NYUSIM. Top view of azimuth plane.

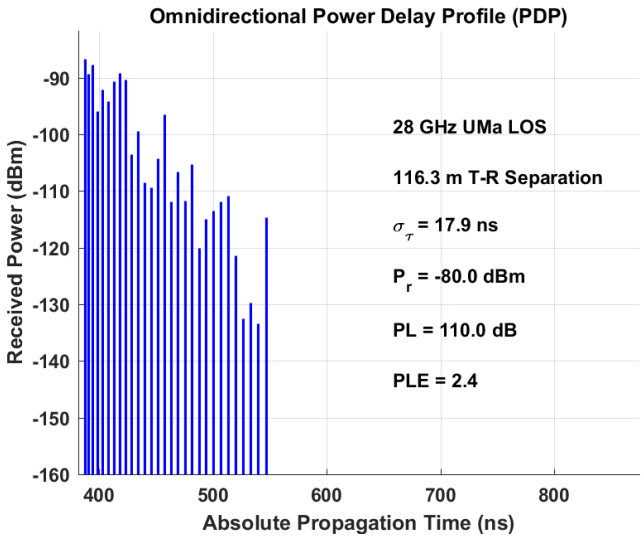

Fig. 1.4.6..3. Sample Omnidirectional PDP generated from NYUSIM.

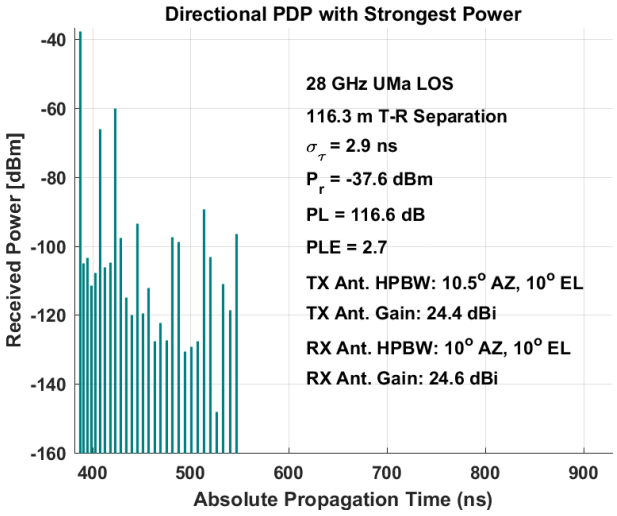

Fig. 1.4.6..4. Sample Directional PDP generated from NYUSIM.

1.5 MmWave and Microwave Model Differences

Due to the increase in frequency, radio waves with high frequency have different propagation characteristics compared to microwave [56]. For example, mmWaves can't efficiently penetrate and diffract around obstacles, e.g., cars, buildings and people. This results in less diffracting MPCs and high path loss. The following subsections focus on

several channel properties in mmWave bands and discuss new requirements for channel models.

1.5.1 Frequency Dependence

MmWave channels have high free space path loss in the first meter of propagation due to its frequency dependence [48]. Furthermore, frequency dependence on other channel parameters, e.g., delay spread and angular spread, also need further investigation. In 3GPP TR 38.901 Release 14 [46], both delay spread and angular spread are modeled as a function of frequency for the channels (except for the rural macro (RMa) scenarios) above 6 GHz.

1.5.2 Attenuation and Blockage

During propagation, mmWaves may be partially or totally absorbed by an absorbing medium, which results in additional loss. Thus, rain attenuation and atmospheric attenuation [57, 58, 59, 60] should be considered in mmWave systems, although this is not a concerned problem in microwave systems. Additionally, mmWave systems are much more sensitive to blockage by obstacles. For example, the path loss increases with the propagation distance. In [61], it was found that outdoor tinted glass had a penetration loss of 40.1 dB at 28 GHz, and three interior walls of an office building had a penetration loss of 45.1 dB, with a distance of 11.39 m between the TX and RX. If stationary or moving objects stand between the TX and RX, channel characteristics will be dramatically changed when the signal is blocked, especially for mmWave channels [62]. The shadowing caused by these objects is important for the link budget and the time variance of the channel. Furthermore, such dynamic blocking is perhaps important to capture in evaluations of technologies, e.g., beam-finding and beam-tracking capabilities.

1.5.3 Channel Sparsity

It is usually claimed that mmWave channels are sparse in the angle and delay domains [2, 63]. For example, in [34], only up to five spatial lobes are found in dense-urban NLOS environments, and the delay/angle spreading within each cluster is relatively small. However, more experimental verifications of this are needed. Nonetheless, a lower bound on the channel sparsity can still be established based on existing measurements, and in many environments the percentage of delay/angle bins with significant energy is rather low while it is higher at centimeter-wave frequencies.

1.5.4 Large Bandwidth and Large Antenna Array

To meet the demand of future mobile data growth [64], bandwidths on the order of 1 GHz are needed. In mmWave bands, there are large bandwidths available. On the other hand, smaller wavelengths make large antenna arrays feasible [65]. Thus, the channel model should consider high resolution in both delay and angular domains. In order to model this effect, the offset angles and relative delay within a cluster should be modeled as variable rather than constant. Various types of antenna arrays, such as the uniform linear array (ULA), uniform rectangle array (URA), and uniform cylinder array (UCA), are being considered. In [66], lens antenna arrays were proposed to enable mmWave MIMO communications. Besides, compared to uniform planar arrays (UPAs), lens antenna arrays can significantly reduce the signal processing complexity and RF chain cost without performance degradation.

1.5.5 Spatial Consistency

Spatial consistency is identified as an important feature for 5G channel models [67]. The spatial consistency of a channel means that the channel evolves smoothly without discontinuities when the TX and/or RX moves or turns. It also means that channel characteristics in closely located users are highly correlated. Spatial consistency covers

various aspects, e.g., large-scale parameters and small-scale parameters of delays, AoAs and AoDs, outdoor/indoor state, and LOS/NLOS state. In [46], a spatial consistency procedure is used for both cluster-specific and ray-specific random variables to be spatially consistent. For example, cluster delays $\tau_n = \tau_{max} X_n$, where τ_{max} is the maximum delay ($2.10^{\mu lgDS + \sigma lgDS}$), Xn is a spatially uniform random variable within (0,1), μlgDS and $\sigma lgDS$ are the mean value and standard deviation of RMS DS respectively.

1.5.6 Stationarity Regions

The study of channel stationarity plays an important role in channel modeling and estimation, since stationarity has to be assumed in order to obtain accurate estimates and reproduce channel parameters. Measurements at 2 GHz to 30 GHz have indicated that the spatial stationarity regions of mmWave bands (less than 0.09 m or so) are much smaller than those at microwave frequencies (around 0.6 m) for an allowance of similarity level of 0.6 [68]. Furthermore, recent field measurements have shown very sharp spatial decorrelation over small distance movements of just a few tens of wavelengths at mmWave frequencies [42], yet it is noteworthy that the orientation of directional antennas with respect to the surrounding environment can impact the stationarity and correlation distances, as demonstrated in [42]. Additionally, the average received power of wideband 73 GHz signals can change by 25 dB as the mobile RX transitioned around a building corner from NLOS to LOS in a UMi scenario [42]. Therefore, stationarity regions need to be carefully characterized in 5G channel modeling that incorporates mmWave bands.

1.5.7 Random Cluster Numbers

In the existing channel model for microwave bands, the number of clusters is a constant [69]. For the mmWave bands, this assumption may not be reasonable. According to recent literature, cluster/time-cluster numbers are small and random, and are well-modeled by a Poisson distribution [63, 34]. In [90], the mean cluster number is 12 while it is less than 4 in [63] (Note that the definition of cluster is different in these two references). By making

the cluster numbers random, some channel properties, e.g., capacity, will change correspondingly.

1.6 Objectives

- To evaluate proper channel parameter for 5G in NLOS and LOS environment at 28 GHz for Urban Micro Cell scenario for Dhaka city
- Analysis of different type of MIMO antenna based on different types of channel and antenna properties for Dhaka city.

That's will be helpful to designing proper channel for 5G wireless communication.

1.7 Motivation

The motivation of this project are as follows:

- 5^{th} Generation Cellular network is the upcoming technology
- It the revolutionary technology in the cellular network
- It creates a lots of technological opportunity
- It planned to deploy with 2020

1.8 Thesis Outline

In this thesis, we described and discussed about our project in chapter 5. The outlines of our thesis are as follows:

- CHAPTER 1: In this chapter the introduction is given and the basic of this thesis has been discussed.

- CHAPTER 2: It contains literature review. All previous work related of this thesis and previous work on mmWave and basics of NYUSIM has been discussed in this chapter.
- CHAPTER 3: It contains the methodology of research work using
- CHAPTER 4: It contains analysis of MIMO for LOS and NLOS Environment for Dhaka city using Urban Microcell and finally inherited the result and discussion.
- CHAPTER 5: It contains conclusion where conclusion and future work has been discussed and references.

1.9 Summary

In this chapter, we are discussing about the upcoming 5G cellular network and the requirements of this upcoming technology. Then implicit about the basic overview of NYUSIM 5G channel simulator that are used to do this research for evaluating performance of MIMO for Dhaka city. Then we clarify about our objective and motivation to do this research and finally short outline of our subsequent chapter.

CHAPTER 2

Literature review

In this chapter, we are explaining about the previous of researcher that are related to this thesis, which is "**Performance evaluation of MIMO in Urban Microcell for Dhaka City at 28 GHz mmWave frequency**". The study of literature review helps to lead to identification the features and weakness of the existing research work.

1) Research paper on "**mmWave frequency**"

The development and growth of wireless technologies in the past decade has led to the rapid adoption of smartphones and tablets, and emerging wearable devices for health and fitness. Consumers are expecting every device they have to be connected to the network to record, transfer, view, or monitor data. With these new technologies comes the demand for more data, video, and content access. While the growth in wireless devices and technologies has sky-rocketed, the spectrum available for these devices has not kept pace. Carriers and other fixed or mobile service providers are reaching the upper bounds of channel capacity, and the reality of a spectrum shortfall is now becoming increasingly clear. The wireless spectrum below 6 GHz will not be enough to meet future needs, as the current global allocation of cellular and unlicensed wireless local area network (WLAN) spectrum is quite small when compared to the vast spectrum available between 6 and 300 GHz [70,71,72,73]. In the past 40 years since the advent of the modern mobile communications industry, clock speeds and memory sizes of communications and computer devices have increased by 4 to 6 orders of magnitude (or more), while the carrier frequencies of all WLAN and cellular networks have increased by less than an order of magnitude, from 450 MHz first generation cellphones, to today's 2 GHz 4G/LTE systems [72],[73].

Wireless systems are increasingly supporting larger and more diverse applications from sensor networks for environmental monitoring, to "smart grid" electrical infrastructures, to

advances in medicine and transportation. To meet this demand, cellular providers need to have access to more bandwidth, which is their primary capital expenditure. They could reduce such costs—and introduce potentially far reaching improvements to cellular access, affordability, and coverage—by making better use of available spectrum in the 30–300 GHz millimeter-wave (mmWave) band are discussed in "**Scenarios for 5G mobile and wireless communications: The vision of the METIS project**" [74].

Also demand in high data rate is on constant rise because of high data rate applications and the anticipated explosive growth in traffic generated by sensors with sensing and communication capabilities in internet of things (IoTs), machine-to machine communication (M2M), vehicle to everything (V2X) communications and smart sensors used in host of other applications are discussed in those paper [75-77]. Furthermore, global data traffic grew 70% from Q1 2016 to Q1 2017 with the trend continuing to increase. It's predicted that traffic demand shall be 1000 times higher in early 2020 than that of traffic in 2010 is mentioned in "**Scaling up mimo: Opportunities and challenges with very large arrays**" [78]. Each new generation of wireless communications demands the search for new spectrum to increase system capacity and to create a ten-fold or more increase in mobile data rates. The limited availability of crowded sub-6 GHz spectrum and the vast amount of unused spectrum at millimeter-wave (mmWave) frequencies many Gigahertz wide band provided motivation for the investigation of mmWave bands for fifth-generation (5G) wireless systems [4, 5].

High capacity, reliable and low-latency and massive connectivity shall be required for 5G mobile communication. The demand in high capacity and low-latency applications can be accommodated by using higher spectrum bandwidth at mmWave frequencies with massive MIMO.

2) Research paper on "**Frequency bands used for 5G cellular network**"

Fifth-generation (5G) cellular systems tend to operate on the centimeter-wave frequency band (3-30 GHz) or millimeter wave frequency band (30 to 100 GHz). MmWave

frequencies have much smaller wavelengths, ranging from 1 mm to 100 mm, about the size of a human fingernail, whereas 4G frequencies have wavelengths that are tens of centimeters. Smaller wavelengths at mmWave frequencies have often been thought to result in higher attenuation (due to oxygen absorption and precipitation) through air, than that observed at today's cellular bands. However, atmospheric attenuation across most of the mmWave spectrum only induces a fraction of a dB to just a few dB of additional loss at a 1 km distance, compared to Ultra High Frequency (UHF) bands [70], [71]. Within the 5G millimeter wave (mmWave), where a vast amount of underutilized bandwidth exists world-wide, mobile radio services, Multiple input multiple-output (MIMO) spatial multiplexing and beamforming are regarded as key technology enablers which was indicated in "**A Flexible Millimeter-Wave Channel Sounder with Absolute Timing**" and "**5G Uniform Linear Arrays with Beamforming and Spatial Multiplexing at 28 37 64 and 71 GHz for Outdoor Urban Communication: A Two-Level Approach**" [79,80].

Smaller wavelengths at mmWave frequencies have often been thought to result in higher attenuation (due to oxygen absorption and precipitation) through air, than that observed at today's cellular bands. It is true that mmWave frequencies undergo greater free space attenuation in the first meter of propagation once leaving an antenna, compared to today's Ultra High Frequency (UHF) cellular frequencies; however, atmospheric attenuation across most of the mmWave spectrum only induces a fraction of a dB to just a few dB of additional loss at a 1 km distance, compared to UHF bands are narrated in those paper [8,9].

Only at certain frequency bands, such as 60 GHz, 180 GHz, or 380 GHz, do molecular resonances create high atmospheric attenuation causing signals to attenuate much more rapidly with distance than today's UHF/microwave bands is mentioned in "**5G wireless backhaul networks: challenges and research advances**" [10]. These high-attenuation mmWave bands are better suited for local or personal area communications, or whisper radios" with coverage distances of a few meters (m) [8]. For precipitation, rain only contributes a few dB of attenuation at mmWaves compared to free space when considering

inter-site base station distances of no more than a few hundred meters, implying that the impact of rain will be mollified through the use of high gain, steerable antennas [10,14].

It can be possible to obtain huge bandwidth in different frequency bands like 28 GHz, 38 GHz,60 GHz and E Band frequency at 71-76 GHz and 81-86 GHz band of millimeter wave band. Many channel have been modelled using these bands. For this work we select 28 GHz band to provide huge bandwidth in our targeted area as our targeted area is densely populated with users and a lot amount of machines which are used for machine to machine communication and also vehicles for vehicle to vehicle or vehicle to everything communications.

3) Research paper on "**Channel modeling for 5th generation cellular network**"

The medium between the transmitting antenna and the receiving antenna is termed as channel. As we know the characteristics of the signal changes when it propagates to transmitter to receiver through channel. There are several causes for this changes like existence of line of sight path between the antennas. Reflection, refraction, diffraction due to the obstacles in between the antennas. The objects between the transmitter and receiver and the relative motion between them. The signal attenuation as it travels through the medium. Noise in the received signal can be obtained from the transmitter signal due to different obstacles. It is quite difficult to design real world environment or scenario of a specific area. Researcher have studied different environment or scenario and provide us with a way to model the various medium that approximate the real world scenario.

Shadowing is a major problem for cannel modeling. If the environment contains objects like building and trees, some part of the transmitted signal is get affected by absorption, reflection, refraction, diffraction and scattering as we talked about them in previous article. It is also referred as slow fading or long term fading [81].

A signal travelling in an environment may get reflected by several objects on the medium. This create chances to different reflected signals. The reflected signals arrive at the receiver at different time instants and with different intensities leading to multipath propagation. Depending on the phase of each individual reflected signal, the power of the received signal may decrease or increase. A small variation in the phase of the each reflected signal from each multipath may lead to significant difference in the total received power. This situation also referred as short term fading or fast fading. The multiple reflected copies of the transmitted signal arrive at the receiver at different power levels and at different time instants. This characteristic of multipath phenomena is described by power delay profile. Power delay profile gives a list of different time delays of each multipath and the associated power levels. This problem should be keep in mind to the researcher when they model a channel for an environment or a scenario in an area.

To properly deploy millimeter, wave in 5G wireless system realistic channel model design is the main challenge for the researcher in the whole worldwide. The construction and implementation of channel models are becoming most important for wireless communication system design, and computer-aided design tools such as channel simulators are essential for performance evaluation of communications systems and for simulating network deployments, before moving forward with new technologies. To properly design and deploy 5G wireless systems, channel models based on fundamental physics and extensive measurements at the corresponding frequency bands are needed to analyze future air interfaces and signaling protocols is presents in "**5G channel model with improved accuracy and efficiency in mmWave bands**" [82].

Channel modelling is an important aspect of design of 5G communication systems particularly outdoor wireless cellular communication. The channel modelling at mmWave is challenging than the legacy sub-6 GHz because of multiple factors including high speed circuits and nonlinear device distortions and because of the wavelength of mmWave band signal. In the paper, "**Statistical channel modelling of 5G mmWave MIMO wireless communication**" the wavelength of signal at mmWave band becomes so small the attenuation caused by water molecules, oxygen, and dust particles present in the air is

paramount, but there is added benefit of reduced antenna size at mmWave band is discussed [83].

The channel modelling at mmWave is challenging than the legacy sub-6 GHz because of multiple factors including high speed circuits and nonlinear device distortions and because of the wavelength of mmWave band signal. The wavelength of signal at mmWave band becomes so small the attenuation caused by water molecules, oxygen, and dust particles present in the air is paramount, but there is added benefit of reduced antenna size at mmWave band [83].

There are several requirements for new channel model that will support 5G millimeter wave frequency bands. Antenna arrays, especially at higher-frequency millimeter-wave bands, will very likely be 2D and dual-polarized both at the access point (AP) and the user equipment (UE) and will hence need properly-modeled azimuth and elevation angles of departure and arrival of multipath components. Individual antenna elements will have antenna radiation patterns in azimuth and elevation and may require separate modeling for directional performance gains. Furthermore, polarization properties of the multipath components need to be accurately accounted for in the model. The new channel model must accommodate a wide frequency range up to 100 GHz. The joint propagation characteristics over different frequency bands will need to be evaluated for multi-band operation, e.g., low-band and high-band carrier aggregation configurations. The new channel model must support large channel bandwidths (up to 2GHz), where, the individual channel bandwidths may be in the range of 100 MHz to 2 GHz and may support carrier aggregation. The operating channels may be spread across an assigned range of several GHz [84].

The new channel model must support a range of large antenna arrays. Some large antenna arrays will have very high directivity with angular resolution of the channel down to around 1.0 degree. 5G will consist of different array types, e.g., linear, planar, cylindrical and spherical arrays, with arbitrary polarization. The array manifold vector can change significantly when the bandwidth is large relative to the carrier frequency. As such, the

wideband array manifold assumption is not valid and new modeling techniques may be required. It may be preferable, for example, to model arrival/departure angles with delays across the array and follow a spherical wave assumption instead of the usual plane wave assumption [84].

The new channel model must accommodate mobility, the channel model structure should be suitable for mobility up to 350 km/hr. The channel model structure should be suitable for small-scale mobility and rotation of both ends of the link in order to support scenarios such as device to device (D2D) or vehicle to vehicle (V2V).

The new channel model must ensure spatial/temporal/frequency consistency, the model should provide spatial/temporal/frequency consistencies which may be characterized, for example, via spatial consistence, inter-site correlation, and correlation among frequency bands. The model should also ensure that the channel states, such as Line of Sight (LOS)/non-LOS (NLOS) for outdoor/indoor locations, the second order statistics of the channel, and the channel realizations change smoothly as a function of time, antenna position, and/or frequency in all propagation scenarios. The spatial temporal frequency consistencies should be supported for simulations where the channel consistency impacts the results (e.g. massive MIMO, mobility and beam tracking, etc. Such support could possibly be optional for simpler studies [84].

The model should be suitable for implementation in single-link simulation tools and in multi-cell, multi-link radio network simulation tools. Computational complexity and memory requirements should not be excessive. Accuracy may be provided by including additional modeling details with reasonable complexity to support the greater channel bandwidths, and spatial and temporal resolutions and spatial/temporal/frequency consistency, required for millimeter-wave modeling. The introduction of a new modeling methodology (e.g. Map based model) may significantly complicate the channel generation mechanism and thus substantially increase the implementation complexity of the system-level simulator. Furthermore, if one applies a completely different modeling methodology

for frequencies above 6 GHz, it would be difficult to have meaningful comparative system evaluations for bands up to 100 GHz [84].

3) Research paper on "**Channel modeling for MIMO**"

For channel modeling MIMO (multiple input multiple output) is very important aspect. Earlier in LTE system MIMO system used. Researcher for millimeter wave bands offering massive MIMO technology which is using orthogonal frequency division multiple access. There are several types of MIMO systems currently in use, with different MIMO radio manufacturers offering their own version of technology with different advantages and unique features. The new generation of small, high performance tactical MIMO radios allows for the benefits of MIMO to be utilize by large groups as well as small organizations. Ad hoc and mesh networking capabilities of many radio systems allows for dynamic deployment and quick response to changing situations without network outages [85].

MIMO radio systems can take advantage of multiple types of antenna polarization schemes to improve diversity, which is one of the key ways MIMO systems are able to provide robust connectivity even challenging environments that would prove difficult for single antenna radio systems. Massive MIMO shall use hundreds of antennas at base station (BS) and provide energy-efficient communication. MIMO radio systems utilize multiple antennas in order to send and receive multiple data streams at once. The number of antennas needed is defined by the radio manufacturer based on what they determine will work for optimal transmission and reception with their particular hardware and software. As for Dhaka city there will be huge more bandwidth so the size of the MIMO should be large. But with the increase of transmitter and receiver there creates some problem. To utilize actual performance, the transmitter should know channel state information, but with the increase of transmitter it is quite difficult to gather these data. These problem is partially solved by using time division duplex system. So for selecting the MIMO antenna these should keep in mind [85].

4) Research paper on "**LOS and NLOS environment in 5G wireless network**"

The LOS path loss in the bands of interest appears to follow Friis' free space path loss model quite well. Just as in lower bands, a higher path loss slope (or path loss exponent) is observed in NLOS conditions. The shadow fading in the measurements appears to be similar to lower frequency bands, while ray-tracing results show a much higher shadow fading (>10 dB) than measurements, due to the larger dynamic range allowed in some ray tracing experiments.

In NLOS conditions at frequencies below 6.0 GHz, the RMS delay spread is typically modelled at around 50-500 ns, the RMS azimuth angle spread of departure (from the AP) at around 10-30°, and the RMS azimuth angle spread of arrival (at the UE) at around 50-80°. There are measurements of the delay spread above 6 GHz which indicate somewhat smaller ranges as the frequency increases, and some measurements show the millimeter wave omnidirectional channel to be highly directional in nature [85]. As we know that Dhaka city is densely with users. Micro cell will be better option to provide proper demand. So we choose UMi as the operating scenario for the new channel.

5) Research paper on "**Channel simulator in 5G wireless network**"

There are several channel simulators that have been developed and used by previous researchers. For instance, Smith [86] built simulation software for indoor and outdoor propagation channels by making use of the two-ray Rayleigh fading channel model developed by Clarke is discussed in "**A statistical theory of mobile-radio reception**" [87]. Fraunhofer Heinrich Hertz Institute developed a 3-D multi-cell channel model that can accurately predict the performance for an urban macrocell setup with commercial high-gain antennas, upon which a channel simulator has been built that supports features such as time evolution, scenario transitions, and so on [88]. A channel simulator for indoor scenarios was developed for machine-to-machine applications [89]. Rappaport and Seidel developed a measurement-based statistical indoor channel model named SIRCIM (Simulation of Indoor Radio Channel Impulse Response Models) for the early development of WiFi [90] and the corresponding simulation software to generate channel impulse responses (CIRs) for indoor channels operating from 10 MHz to 60 GHz. A similar open-

source RF propagation simulator is SMRCIM (Simulation of Mobile Radio Channel Impulse Response Models), that was useful for simulating outdoor channels [91], [92]. Another software simulation program, called BERSIM [93], developed by Fung et al., was able to simulate mobile radio communication links and calculate average bit error rate (BER) and bit-by-bit error patterns, that was useful for evaluating link quality in real time without requiring any radio frequency hardware.

Among the existing channel models, there are two main types of channel models now being considered by researchers and the industry for 5G wireless: one is the channel model inherited from the model for sub-6 GHz communication systems with modifications to accommodate the spectrum above 6 GHz up to 100 GHz, such as the 3GPP and ITU channel models; the other is the model established based also on extensive propagation measurements at frequencies from 0.5 to 100 GHz, such as NYUSIM developed based on millimeter-wave (mmWave) field measurements [94], [98]–[102].

NYUSIM has been developed based on extensive real-world wideband propagation channel measurements at multiple millimeter-wave (mmWave) frequencies from 28 to 73 GHz in various outdoor environments in urban microcell (UMi), urban macrocell (UMa), and rural macrocell (RMa) environments [103] – [111]. NYUSIM provides an accurate rendering of actual channel impulse responses in both time and space, as well as realistic signal levels that were measured, and is applicable for a wide range of carrier frequencies from 500 MHz to 100 GHz, and RF bandwidths from 0 to 800 MHz. As of early 2017, over 7,000 downloads of NYUSIM have been recorded. The source code was written in MATLAB [20] and a platform-independent graphical user interface (GUI) was created to facilitate the use of NYUSIM on machines using either Windows or Macintosh operating systems even without MATLAB installed.

Omnidirectional channel models have widely been studied and adopted by industry and researchers around the world to assist in wireless system design, yet directional channel models are also important to properly design and implement antenna arrays to exploit

spatial diversity and/or beamforming gain in multiple-input multiple-output (MIMO) systems [112], [113].

This software based on statistical spatial channel model (SSCM) is backed by extensive measurements at mmWave frequencies. It uses time clusters (TCs) and spatial lobes to generate channel impulse responses and respective angle of arrival (AoA)/angle of departure (AoD) power spectra [12]. Time clusters are multipath components (MPCs) tightly packed in time that arrive from different directions. This software powered by SSCM can receive MPCs in a time cluster arriving from different angles because of high gain antennas and such feature is not available in 3GPP and WINNER propagation models[13][14]. This software can be used to generate channel impulse response (CIRs) for mmWave systems, perform BER simulation, characterise MIMO channel and obtain MIMO channel condition number. Condition number is a ratio of the highest and lowest value in singular value decomposition matrix (SVD) of MIMO channel [71].

Statistical channel modeling for 5G mmWave wireless communication multiple input multiple output has been considered with one two element transmitter and two element receivers at four instants. Lower bound and upper bound on transmitter and receiver separation is 100m to 120 m. The underlying scenario has been evaluated in terms of received power, path loss exponent (PLE) and path loss for directional, best-directional and omnidirectional cases.U.S. national institute for standards and technologies (NIST) 5G mmWave signal characterization and analyses for device measurements for mmWave and cellular applications are notable. NIST measurements are targeted for mmWave signal characterization, traceability of wideband modulated signals, integrated antenna arrays, uncertainties measurements in error vector magnitude (EVM), nonlinear mmWave device measurements and calibration, over-the-air (OTA) testing for massive MIMO, digital beamforming testbeds, reverberation chamber OTA measurements etc. Channel sounder-system has been developed to access the MPCs to extract information on path loss, delay, AoA at mmWave frequencies. Pathloss for specific transmit-receive set up at 83.5 GHz for LOS and NLOS scenarios for indoor environment has been measured [23].

Because of the necessity of huge amount of data for Dhaka city new channel modelling has become mandatory in 5G wireless communication. There are a lot of requirements to design a new channel for a particular area either it can be urban or rural. By focusing on the amount of user's microcell or macrocell should be determined. To fulfill the requirement our channel simulator offering more realistic data comparison with other channel simulator. Hopefully, 5G will be officially planned to launch in 2020. Then that time to determine proper channel parameter for designing channel will be going to be highly significant.

Chapter 3

Methodology

3.1 Methodology

Methodology is a set of practices. This term may be used to refer to practices which are widely used across in industry or scientific discipline, the techniques used in a particular research study, or the techniques used to accomplish a particular project. People may also use the term "methodology" to refer to the study of such methods, rather than the methods themselves.

A methodology can be considered to include multiple methods, each as applied to various facts of the whole scope of the methodology. The research can be divided between two parts, they are qualitative research and quantitative research.

3.2 Research Design

Research design is the framework that has been created to seek answers to research question. The design of a study defines the research material such as research question. The design of a study defines the research materials such as research question, independent and a dependent variable, experimental design, and if applicable, data collection methods and a statistical analysis plan. Research design for this research:

- Study on 5G cellular network
- Study on mmWave band frequency
- Study on MIMO
- Study on Channel modeling
- Study on Channel modeling parameter
- Study on Power delay profile
- Study on LOS and NLOS environment communication
- Study on AoA and AoD parameter for channel design
- Study on the environment on Dhaka city
- Study on the Urban Microcell

- Find out the proper channel parameter for channel design
- Implement the procedure

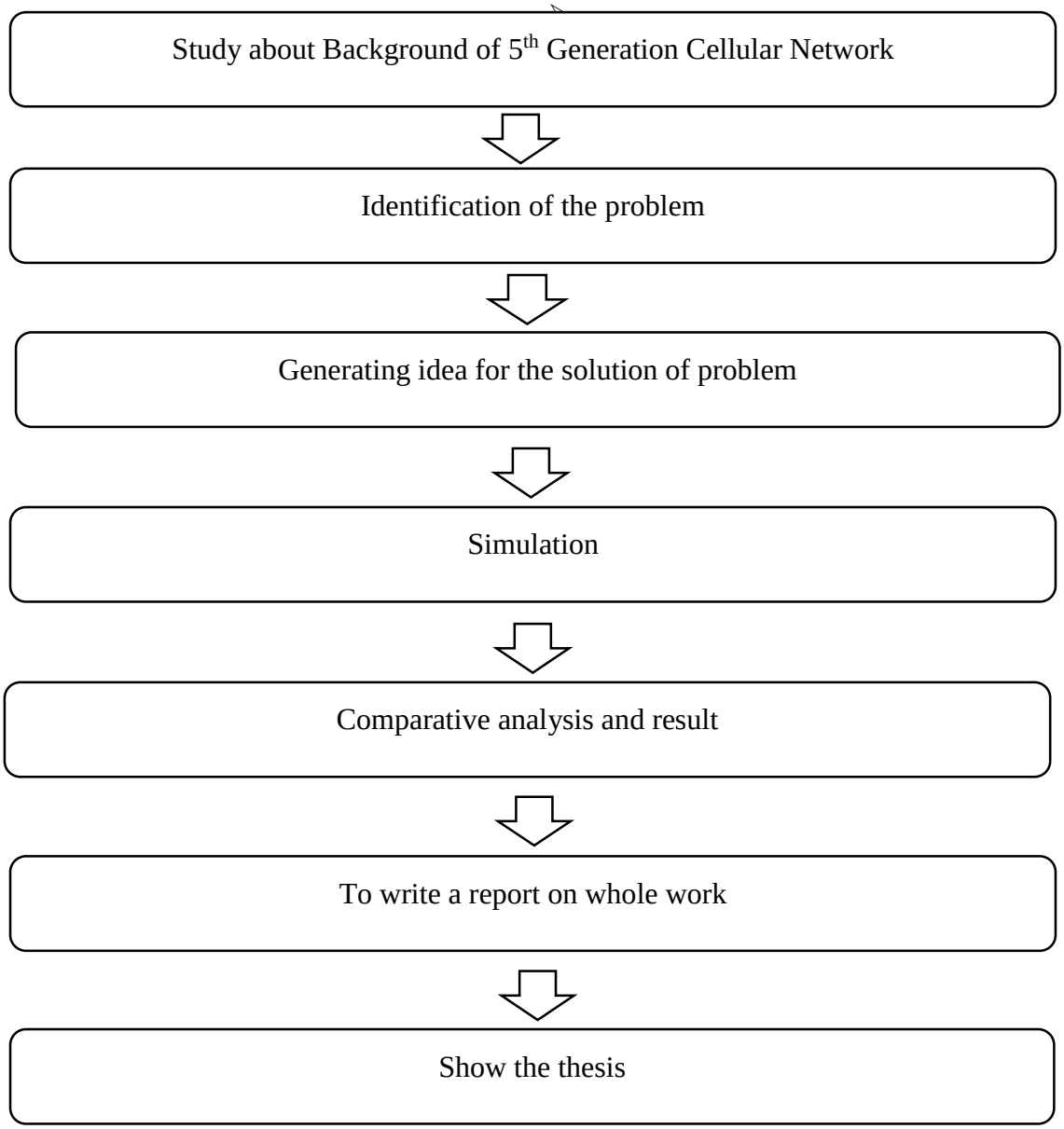

Fig. 3.2.1. A block diagram of overview of whole research

3.3 Pilot Study

Pilot studies are small-scale, preliminary studies which aim to investigate whether crucial components of a main study – usually a randomized controlled trial (RCT) – will be feasible. For example, they may be used in attempt to predict an appropriate sample size for the full-scale project and/or to improve upon various aspects of the study design. Often RCTs require a lot of time and money to be carried out, so it is crucial that the researchers have confidence in the key steps they will take when conducting this type of study to avoid wasting time and resources.

Thus, a pilot study must answer a simple question: "**Can the full-scale study be conducted in the way that has been planned or should some component(s) be altered?**"

The reporting of pilot studies must be of high quality to allow readers to interpret the results and implications correctly. This blog will highlight some key things for readers to consider when they are appraising a pilot study.

- Main reasons of Pilot study:

Pilot studies are conducted to evaluate the feasibility of some crucial component(s) of the full-scale study. Typically, these can be divided into 3 main aspects:

- **Process:** where the feasibility of the key steps in the main study is assessed
- **Resources:** assessing problems with time and resources that may occur during the main study (e.g. how much time the main study will take to be completed; whether use of some equipment will be feasible or whether the form(s) of evaluation selected for the main study are as good as possible)
- **Management:** problems with data management and with the team involved in the study (e.g. whether there were problems with collecting all the data needed for future analysis; whether the collected data are highly variable and whether data from different institutions can be analyzed together).

3.4 Software

NYUSIM 5G channel simulator and MATLAB 2018

3.5 Procedure

Step 1: At first we are studying on the 5^{th} generation cellular network, mmWave band frequency, MIMO, NLOS and LOS environment, channel modeling on the 5^{th} generation network.

Step 2: Then studying on the parameter for channel modeling and urban microcell.

Step 3: Then collect data for channel and antenna properties Dhaka city that are used in current network.

Step 4: Then simulate the MIMO for specific condition based on real environment data for 28 GHz frequency.

Step 5: Save the result.

Step 6: Analysis the result.

Step 7: Identify the proper channel parameter for best MIMO antenna.

Step 8: Write down a report based on whole research work.

3.6 Allocation of Rain Rate for Dhaka City

The yearly statistics of rainfall for the last 23 years (1993 - 2013) of Dhaka city are amassed from Meteorological Department of Bangladesh. As a subtropical country, heavy rainfall is characteristic of Bangladesh. If we analysis the data of last 23 years, Dhaka city receive at least 2000 mm of rainfall per year. And if we average all of the rainfall of this data, we can allocate averagely 110mm/hr. rainfall for Dhaka city.

TABLE 3.6.1 Allocation of Rain Rate for Dhaka City [120]

Year	JAN	FEB	MAR	APR	MAY	JUN	JUL	AUG	SEP	OCT	NOV	DEC
1993	5	53	87	113	556	486	418	439	374	217	19	0
1994	13	54	115	201	254	266	153	246	169	55	14	0
1995	8	31	0	88	264	237	354	360	205	91	112	1
1996	0	21	54	199	208	343	257	361	244	357	0	0
1997	2	7	136	133	151	249	549	230	402	39	1	22
1998	49	4	83	178	405	91	521	552	246	100	83	0
1999	0	0	0	21	428	348	553	282	361	368	13	0
2000	13	44	172	189	471	192	200	426	214	272	0	0
2001	0	1	33	46	402	392	202	205	209	177	18	0
2002	24	4	51	111	272	373	446	272	144	52	40	0
2003	0	25	96	123	140	473	191	202	264	134	0	45
2004	0	0	9	167	162	476	295	191	839	208	0	0
2005	1	3	155	91	291	259	542	361	514	417	3	0
2006	0	0	0	181	185	326	331	167	663	61	5	0
2007	0	30	11	163	185	628	753	505	179	320	111	0
2008	23	56	45	91	205	577	563	319	279	227	0	0
2009	1	1	43	14	168	170	676	482	298	74	4	0
2010	0	48	22	37	177	308	167	340	169	174	0	81
2011	0	0	20	123	235	314	356	409	207	112	0	0
2012	10	1	37	269	137	175	226	282	81	38	68	5
2013	0	8	26	32	378	325	302	212	172	131	0	4

3.7 Allocation of Relative Humidity (Percent) for Dhaka City

Humidity is the amount of water vapor present in the air. Water vapor is the gaseous state of water and is invisible to the human eye. Humidity indicates the likelihood of precipitation, dew, or fog. Bangladesh has a subtropical monsoon climate characterized by wide seasonal variations in rainfall, high temperatures and humidity. There are three distinct seasons in Bangladesh: a hot, humid summer from March to June; a cool, rainy

monsoon season from June to October; and a cool, dry winter from October to March. The ideal relative humidity for health and comfort is about 40–50%. But in Dhaka city it was averaged 65%.

TABLE 3.7.1 Allocation of Relative Humidity for Dhaka City [120,121]

YEAR	JAN	FEB	MAR	APR	MAY	JUN	JUL	AUG	SEP	OCT	NOV	DEC
1993	73	69	62	70	80	82	84	85	83	82	79	75
1994	69	67	65	70	76	81	79	81	78	74	71	65
1995	64	66	58	64	75	81	82	82	82	78	74	70
1996	73	67	67	70	78	83	84	85	83	79	76	72
1997	70	64	66	75	77	82	86	84	86	78	75	80
1998	77	68	64	75	78	81	87	86	85	82	78	77
1999	72	65	57	69	79	83	86	84	84	83	76	71
2000	72	61	63	73	78	80	80	81	81	82	73	69
2001	63	62	56	67	79	84	82	82	83	81	78	75
2002	68	58	58	73	79	84	85	82	79	75	74	74
2003	75	66	65	71	73	82	80	79	83	81	67	73
2004	74	61	63	73	68	82	82	79	86	75	70	71
2005	69	61	67	67	74	80	82	83	82	81	73	67
2006	69	66	54	68	73	82	80	78	81	77	69	70
2007	68	69	55	70	71	81	85	81	81	79	78	70
2008	70	62	68	65	71	81	84	82	81	78	70	80
2009	72	55	53	66	72	75	80	82	81	73	67	70
2010	72	57	59	67	72	79	77	79	80	75	69	66
2011	69	55	58	65	76	81	79	83	77	74	68	73
2012	66	52	58	70	70	78	80	79	79	72	68	77
2013	65	56	55	64	79	77	78	81	81	79	67	73

3.8 Allocation of Barometric Pressure for Dhaka City

Barometric pressure, also known as atmospheric pressure, is the weight of every air molecule above us, reaching all the way to the edge of space. Barometric pressure can affect a variety of things in our environment. These can include the oxygen content in our oceans, lakes, and rivers, water levels, our health, and the weather. Since barometric pressure plays such an important role in our daily lives, we use devices called barometers

to keep us informed of changes in barometric pressure. By analysis of 12 days' data of April 2018, the average barometric pressure for Dhaka city is averaged 1013 mbar.

TABLE 3.8.1 Allocation of Barometric Pressure for Dhaka City [122]

07 April	**08 April**	**09 April**	**10 April**	**11 April**	**12 April**	**13 April**	**14 April**	**15 April**	**16 April**	**17 April**	**18 April**
1009.8 mbar	1013 mbar	1013 mbar	1013 mbar	1013 mbar	1013 mbar	1013 mbar	1013 mbar	1013 mbar	1013 mbar	1013 mbar	1013 mbar

3.9 Allocation of Temperature for Dhaka City

A UHI is a metropolitan area which is significantly warmer than its surrounding rural areas. The temperature difference usually is larger at night than during the daytime and larger in winter than in summer, and is most apparent when winds are weak. The main cause of the urban heat island is modification of the land surface by urban development; waste heat generated by energy usage is a secondary contributor. Since we have covered most of the land surface of Dhaka with concrete and asphalt pavements, the city has become an oven with millions of people in it. The average temperature for Dhaka city is roaming within 20-30 degree celsius by analysis of 23 years' data that are getting from meteorological station of Bangladesh.

TABLE 3.9.1 Allocation of Temperature for Dhaka City [120]

JAN	**FEB**	**MAR**	**APR**	**MAY**	**JUN**	**JUL**	**AUG**	**SEP**	**OCT**	**NOV**	**DEC**
18.8	22.4	26.8	28.9	29.3	29.5	29.2	29.3	29.1	27.9	24.6	20.7

3.10 Procedure of calculating path loss

From (1) and (2), along with other research in [116], and [117], path loss can be derived to include dependence on frequency as

$$\overline{PLM(d_0 f)}(\text{dB}) = \alpha + \bar{\beta} \cdot 10log_{10}(d_0) + \gamma \cdot 20log_{10}(\frac{f}{f_c}) \quad (3.10.1)$$

where γ represents a frequency dependency factor, and f/fc is the ratio of frequency deviation from the carrier frequency. $\bar{\beta}$ represents an extracted best-fit linear regression to (3.10.1) using path loss values which are computed from the previous section's PDPs by integrating each point to obtain received signal power at each location and AOD, then normalizing to the transmitted power of 30 dBm. The approach used to calculate

$\bar{\beta}$ can be described by

$$\bar{\beta} = \frac{\sum_i^n (d_i - \overline{d_0}) \times (PLM_i - \overline{PLM})}{\sum_i^n (d_0 - \bar{d})^2} \quad (3.10.2)$$

which is an adaptation of the work found in [118] where d_i is the distance (in dB scale) of the ith measurement of PDPs for a given AOD and RX location. $\overline{d_0}$ is the average distance for all d_i from the simulated value, and PLM is the average path loss for the data set. Moreover, here, α represents a floating intercept, as described by [118], of the linear regression fit for (3.10.1) and, thus, (3.10.2), which can fit data through examination, determines an attenuation point that can be used for the path loss model. α can be determined by

$$\alpha(\text{dB}) = \overline{PLM}\ (\text{dB}) - \bar{\beta} \cdot 10log_{10}(d_0). \quad (3.10.3)$$

For the linear regression, the value for α and $\bar{\beta}$ are solved in parallel form (3.10.2) and (3.10.3). The regression fit has been computed for both the set of five transmissions on the 28 GHz and GHz frequencies.

Chapter 4

Analysis, Simulation and Result

4.1 Analysis of MIMO for NLOS Environment for Dhaka city using Urban Microcell

4.1.1 Analysis of MIMO using different T-R separation distance for urban microcell

The technique of Multiple-input multiple-output (MIMO) have been used in modern wireless communication to improve reliability and capacity. The multiple antennas in a MIMO system may be deployed in different ways. The selection of right antenna element for MIMO is important for achieving better received power and less path loss for specific distance.

At first we are calculating data for Dhaka city in NLOS environment at some fixed condition for evaluating proper number of antenna element for MIMO. Table 4.1.1.1 and 4.1.1.2 is for 100 m T-R separation distance, then Table 4.1.1.3 and 4.1.1.4 is for 300m distance and finally Table 4.1.15 and 4.1.16 is for 500m distance respectively for omnidirectional and directional antenna.

- Average Rain Rate for Dhaka city: 110mm/hr.
- Average Barometric Pressure for Dhaka city: 1013 mbar [121]
- Average Humidity for Dhaka city: 65% [120,122]
- Temperature: 20^0 Celsius
- Number of receiver location: 100
- Scenario: Urban Micro Cell
- Transmitter power: 30 dBm
- Array type: Uniform Rectangular Array

TABLE 4.1.1.1 Path Loss, Received Power and RMS Delay Spread for 28 GHz NLOS scenario at 100m distance for Omnidirectional antenna

MIMO Used	Path Loss Exponent	Path Loss in dB	Received Power in dBm	RMS Delay Spread in ns
2*2	3.9	140.3	-110.3	11.4
3*3	3.5	132.2	-102.2	19.1
4*4	3.1	122.6	-92.6	9.1
5*5	3.2	125.1	-95.1	9.8
6*6	3.1	122.6	-92.6	32.1
7*7	2.9	118.7	-88.7	25.7

TABLE 4.1.1.2 Path Loss, Received Power and RMS Delay Spread for 28 GHz NLOS scenario at 100m distance for directional antenna

MIMO Used	Path Loss Exponent	Path Loss in dB	Received Power in dBm	RMS Delay Spread in ns
2*2	4.2	146.1	-66.9	0.1
3*3	3.7	134.7	-55.5	3.7
4*4	3.1	123.7	-44.5	0.4
5*5	3.4	129.2	-50.0	0.3
6*6	3.2	125.1	-49.9	7.6
7*7	2.9	119.5	-40.3	0.7

TABLE 4.1.1.3 Path Loss, Received Power and RMS Delay Spread for 28 GHz NLOS scenario at 300m distance for Omnidirectional antenna

MIMO Used	Path Loss Exponent	Path Loss in dB	Received Power in dBm	RMS Delay Spread in ns
2*2	3.4	144.7	-114.7	30.1
3*3	3.5	148.4	-118.4	26.4
4*4	3.2	140.5	-110.5	16.6
5*5	3.7	152.1	-122.1	47.0
6*6	3.1	138.4	-108.4	38.4
7*7	3.6	149.6	-119.6	24.0

TABLE 4.1.1.4 Path Loss, Received Power and RMS Delay Spread for 28 GHz NLOS scenario at 300m distance for directional antenna

MIMO Used	Path Loss Exponent	Path Loss in dB	Received Power in dBm	RMS Delay Spread in ns
2*2	3.6	150.2	-71.0	5.8
3*3	3.7	152.3	-73.1	1.8
4*4	3.5	147.9	-68.7	0.2
5*5	3.9	158.4	-79.2	14.7
6*6	3.2	141.0	-61.8	3.4
7*7	3.7	153.4	-74.2	7.7

TABLE 4.1.1.5 Path Loss, Received Power and RMS Delay Spread for 28 GHz NLOS scenario at 500m distance for Omnidirectional antenna

MIMO Used	Path Loss Exponent	Path Loss in dB	Received Power in dBm	RMS Delay Spread in ns
2*2	3.3	151.0	-121.0	20.2
3*3	3.2	147.3	-117.3	41.8
4*4	3.1	144.4	-114.4	35.0
5*5	3.7	161.3	-131.3	52.5
6*6	3.5	156.2	-126.2	38.9
7*7	3.8	163.7	-133.7	40.6

TABLE 4.1.1.6 Path Loss, Received Power and RMS Delay Spread for 28 GHz NLOS scenario at 500m distance for directional antenna

MIMO Used	Path Loss Exponent	Path Loss in dB	Received Power in dBm	RMS Delay Spread in ns
2*2	3.4	153.3	-74.1	1.2
3*3	3.3	150.6	-71.4	3.0
4*4	3.3	149.6	-70.3	5.3
5*5	3.8	164.8	-85.6	15.1
6*6	3.6	159.9	-80.7	4.0
7*7	3.9	166.4	-87.2	6.1

From the analysis of above calculation of that's type of data we can indicate that the MIMO with 4*4 antenna element is giving less path loss, better received power and less RMS delay spread. And also can able to say, directional path loss and directional PLE will always be larger (i.e., a directional channel is more lossy) than the omnidirectional case, because the directional antenna will spatially filter out many multipath components due to its directional pattern, such that the RX receives fewer multipath components hence less energy, thereby the directional path loss is higher after removing the antenna gain effect from the received power. This indication is true from small to larger distance. We are doing this calculation for 100m, 300m and 500m T-R separation distance. And each of simulation time 4*4 MIMO will give us definitely good result if we compare with other MIMO antenna element.

4.1.2 Analysis of 4*4 MIMO using different T-R separation distance and Temperature for NLOS environment

As Bangladesh is a subtropical country, the season is not always remaining same in the year. In the time of sunny days' temperature will increase up to 35^0 to 39^0 Celsius as per as last 3-5 year records. It will averagely 30^0 Celsius in that time.

So, now we are calculating data for NLOS environment at temperature 30 degree Celsius with 0mm/hr. rain rate

- Average Rain Rate for Dhaka city: 0 mm/hr.
- Average Barometric Pressure for Dhaka city: 1013 mbar [121]
- Average Humidity for Dhaka city: 65% [120,122]
- Temperature: 30^0 Celsius
- Number of receiver location: 100
- Scenario: Urban Micro Cell
- Transmitter power: 30 dBm
- Array type: Uniform Rectangular Array

TABLE 4.1.2.1 Path Loss, Received Power and RMS Delay Spread for 28 GHz NLOS scenario at 30^0 Celsius for Omnidirectional antenna

T-R Separation in m	PLE	Path Loss in dB	Received Power in dBm	RMS Delay Spread in ns
100	3.8	138.2	-108.2	11.4
300	3.4	145.5	-155.5	19.1
500	3.0	143.0	-113.0	9.1

TABLE 4.1.2.2 Path Loss, Received Power and RMS Delay Spread for 28 GHz NLOS scenario 30^0 Celsius for directional antenna

T-R Separation in m	PLE	Path Loss in dB	Received Power in dBm	RMS Delay Spread in ns
100	4.1	144.0	-64.8	0.1
300	3.5	148.0	-68.7	3.7
500	3.1	144.0	-64.9	0.4

Table 4.1.2.1 shows the channel parameter specially path loss exponent, received power and rms delay spread for omnidirectional antenna and Table 4.1.2.1 is for directional antenna. And it's definitely true that at the temperature 30^0 celsius, with the increasing of distance between transmitter and receiver the average path loss will be decreased and the received will be increased for receiver location 1 to 3 both for omnidirectional and directional antenna. And we are able to say, in the high temperature 4*4 MIMO antenna will provide better result in the long distance.

- As we are saying previously, Bangladesh is a subtropical country, in the season of winter the temperature is generally below 20^0 or below 20^0 and also there is no heavy rainfall.

So, at now we are using 15-degree temperature for calculating data:

- Average Rain Rate for Dhaka city: 0 mm/hr.
- Average Barometric Pressure for Dhaka city: 1013 mbar [121]
- Average Humidity for Dhaka city: 65% [120,122]

- Temperature: 15^0 Celsius
- Number of receiver location: 100
- Scenario: Urban Micro Cell
- Transmitter power: 30 dBm
- Array type: Uniform Rectangular Array

TABLE 4.1.2.3 Path Loss, Received Power and RMS Delay Spread for 28 GHz NLOS scenario at 15^0 Celsius for Omnidirectional antenna

T-R Separation in m	**PLE**	**Path Loss in dB**	**Received Power in dBm**	**RMS Delay Spread in ns**
100	3.3	128.4	-98.4	24.0
300	2.9	132.5	-102.5	38.4
500	3.4	153.2	-123.6	5.9

TABLE 4.1.2.4 Path Loss, Received Power and RMS Delay Spread for 28 GHz NLOS scenario at 15^0 Celsius for directional antenna

T-R Separation in m	**PLE**	**Path Loss in dB**	**Received Power in dBm**	**RMS Delay Spread in ns**
100	3.5	132.2	-53.0	7.7
300	3.0	135.1	-55.9	3.4
500	3.5	156.2	-77.0	0.4

So, from Table 4.1.2.3 and 4.1.2.4, we can able to say that when temperature is low and there is no rainfall, 4*4 MIMO antenna will show clearly better result when the T-R separation distance is near 300m. So with the decreasing of temperature we also need to decrease the distance between transmitter and receiver for achieving better output. And also we can to say, the effect of rain is so much drastic for which path loss will be increased.

4.2 Analysis of MIMO for LOS Environment for Dhaka city using Urban Microcell

4.2.1 Analysis of MIMO using different T-R separation distance for LOS environment

The mobile industry has found benefit in describing path loss for both LOS and NLOS conditions separately. As a consequence, models for the probability of LOS are required, i.e., statistical models are needed to predict the likelihood that a UE is within a clear LOS of the BS, or in an NLOS region due to obstructions. LOS propagation will offer more reliable performance in mmWave communications as compared to NLOS conditions, given the greater diffraction loss at higher frequencies and given the larger path loss exponent as well as increased shadowing variance in NLOS as compared to LOS. The LOS probability is modeled as a function of the 2D TX-RX (T-R) separation distance and is frequency-independent, as it is solely based on the geometry and layout of an environment or scenario [23]. In the approach of 5GCM [12], the LOS state is determined by a map-based approach in which only the TX and the RX positions are considered for determining if the direct path between the TX and RX is blocked.

So, now we are calculating data for Dhaka city in LOS environment at some fixed condition. In here we are choosing the summer season for MIMO selection where there is no rain and the temperature is raising up to average 30^0 Celsius.

- Average Rain Rate for Dhaka city: 0mm/hr.
- Average Barometric Pressure for Dhaka city: 1013 mbar [121]
- Average Humidity for Dhaka city: 65% [120,122]
- Temperature: 30^0 Celsius
- Number of receiver location: 100
- Scenario: Urban Micro Cell
- Transmitter power: 30 dBm
- Array type: Uniform Rectangular Array

TABLE 4.2.1.1 Path Loss, Received Power and RMS Delay Spread for 28 GHz LOS scenario at 100m T-R separation distance for omnidirectional antenna

MIMO	PLE	PL in dB	Received Power in dBm	RMS Delay Spread in ns
2*2	2.4	108.7	-78.7	17.9
3*3	2.0	101.3	-71.3	21.9
4*4	1.9	98.6	-68.6	15.8
5*5	2.0	100.4	-70.4	20.4
6*6	2.1	104.2	-74.2	15.0

TABLE 4.2.1.2 Path Loss, Received Power and RMS Delay Spread for 28 GHz LOS scenario at 100m T-R separation distance for directional antenna

MIMO	PLE	PL in dB	Received Power in dBm	RMS Delay Spread in ns
2*2	2.7	115.3	-36.1	2.9
3*3	2.3	107.0	-27.7	6.5
4*4	2.1	102.8	-23.6	0.9
5*5	2.2	105.2	-26.0	6.0
6*6	2.3	107.1	-27.9	0.3

TABLE 4.2.1.3 Path Loss, Received Power and RMS Delay Spread for 28 GHz LOS scenario at 300m T-R separation distance for omnidirectional antenna

MIMO	PLE	PL in dB	Received Power in dBm	RMS Delay Spread in ns
2*2	2.1	114.3	-84.3	20.2
3*3	1.9	108.1	-78.1	16.8
4*4	2.4	120.4	-90.4	12.3
5*5	2.0	110.9	-80.9	13.2
6*6	2.1	112.4	-82.4	19.5

TABLE 4.2.1.4 Path Loss, Received Power and RMS Delay Spread for 28 GHz LOS scenario at 300m T-R separation distance for directional antenna

MIMO	PLE	PL in dB	Received Power in dBm	RMS Delay Spread in ns
2*2	2.4	120.1	-40.9	2.6
3*3	2.1	114.4	-35.2	1.4
4*4	2.6	125.0	-45.8	1.4
5*5	2.2	115.4	-36.2	2.6
6*6	2.3	118.2	-39.0	2.5

TABLE 4.2.1.5 Path Loss, Received Power and RMS Delay Spread for 28 GHz LOS scenario at 500m T-R separation distance for omnidirectional antenna

MIMO	PLE	PL in dB	Received Power in dBm	RMS Delay Spread in ns
2*2	2.0	115.9	-85.9	21..2
3*3	1.9	113.5	-83.5	24.0
4*4	1.5	100.6	-70.6	13.8
5*5	1.9	112.5	-82.5	18.7
6*6	2.1	116.7	-86.7	17.8

TABLE 4.2.1.6 Path Loss, Received Power and RMS Delay Spread for 28 GHz LOS scenario at 500m T-R separation distance for directional antenna

MIMO	PLE	PL in dB	Received Power in dBm	RMS Delay Spread in ns
2*2	2.3	122.3	-43.1	3.8
3*3	2.0	115.0	-35.8	0.5
4*4	1.6	105.1	-25.9	1.2
5*5	2.1	116.8	-37.6	1.0
6*6	2.2	120.1	-40.9	0.4

In the LOS environment, the selection of right antenna element for MIMO is not so easy. Because of in this environment, the value of path loss, received power shows fluctuation

for different types of MIMO. But after that, we can say 4*4 MIMO antenna again show averaged better received power, less path loss and less RMS delay spread. When we are increasing antenna element, there are need to face some problem. Like, the first one is essential for the transmitter to acquire the Channel State Information (CSI) to fully enjoy the capacity gain offered by MIMO systems, especially for multi-user scenarios. However, as the number of antennas increases, the overhead of acquiring CSI grows accordingly. This issue can be partially solved in a Time Division Duplex (TDD) system which reduces the overhead of CSI by utilizing the reciprocity of the channel.

And then another major problem, which was pointed out that the complexity of precoding and detection will rise with the number of antennas. When the number of transmit antennas is much larger than the number of receive antennas, simple linear precoders and detectors are sufficient to offer nearly optimal performance. However, when the number of transmit antennas is comparable to or less than the number of receive antennas, the design of precoders and detectors with reasonable complexity becomes more challenging.

So, we can say, that's the reason for which large type of MIMO antenna is expressed less good result.

4.2.2 Analysis of 4*4 MIMO using different T-R separation distance and Temperature for NLOS environment

Now we are calculating data for LOS environment at temperature 15^0 Celsius with 0mm/hr. rain rate

- Average Rain Rate for Dhaka city: 0 mm/hr.
- Average Barometric Pressure for Dhaka city: 1013 mbar [121]
- Average Humidity for Dhaka city: 65% [120,122]
- Temperature: 15^0 Celsius
- Number of receiver location: 100
- Scenario: Urban Micro Cell
- Transmitter power: 30 dBm
- Array type: Uniform Rectangular Array

TABLE 4.2.1 Path Loss, Received Power and RMS Delay Spread for 28 GHz LOS scenario at 15^0 Celsius for Omnidirectional antenna

T-R Separation in m	PLE	Path Loss in dB	Received Power in dBm	RMS Delay Spread in ns
100	2.4	108.7	-78.7	17.9
300	2.0	110.8	-80.8	21.9
500	1.9	112.7	-82.7	15.8

TABLE 4.2.2 Path Loss, Received Power and RMS Delay Spread for 28 GHz LOS scenario at 15^0 Celsius for directional antenna

T-R Separation in m	PLE	Path Loss in dB	Received Power in dBm	RMS Delay Spread in ns
100	2.7	115.3	-36.1	2.9
300	2.2	116.5	-37.3	6.5
500	2.1	116.8	-37.6	0.9

In this condition of LOS environment, it will show gradual result, like with the increase of receiver location 4*4 MIMO antenna will show better result for lower transmitter receiver separation distance. Like that, when the receiver location is set to 1, then the MIMO antenna will provide better result for 500m T-R separation distance. And when the receiver location is 3, then this distance is gradually decrease to 100m both for directional and omnidirectional antenna. And it also different from NLOS environment. In NLOS environment, when temperature is low and there is no rainfall, 4*4 MIMO antenna will show probably better result when the T-R separation distance is near 300m and there is no dependency in receiver location.

- So, now with 20^0 Celsius and 100mm/hr. rain rate the calculation for LOS environment is goes to,

- Average Rain Rate for Dhaka city: 110 mm/hr.
- Average Barometric Pressure for Dhaka city: 1013 mbar [121]
- Average Humidity for Dhaka city: 65% [120,122]
- Temperature: 20^0 Celsius
- Number of receiver location: 100
- Scenario: Urban Micro Cell
- Transmitter power: 30 dBm
- Array type: Uniform Rectangular Array

TABLE 4.2.3 Path Loss, Received Power and RMS Delay Spread for 28 GHz NLOS scenario at 20^0 Celsius for Omnidirectional antenna

T-R Separation in m	**PLE**	**Path Loss in dB**	**Received Power in dBm**	**RMS Delay Spread in ns**
100	2.5	110.7	-80.7	17.9
300	2.2	116.8	-86.8	21.9
500	2.3	122.5	-92.5	15.8

TABLE 4.2.4 Path Loss, Received Power and RMS Delay Spread for 28 GHz NLOS scenario at 20^0 Celsius for directional antenna

T-R Separation in m	**PLE**	**Path Loss in dB**	**Received Power in dBm**	**RMS Delay Spread in ns**
100	2.8	117.3	-38.1	2.9
300	2.5	122.4	-43.2	6.5
500	2.4	126.7	-47.5	0.9

In, the LOS environment, there is not so much effect of rain in the wireless communication which will be assure by those table. Those calculations also indicate that, when the receiver location increase that means N simulation runs are performed to emulate N random MIMO

channel realizations with the input parameters described above. And, also there is in low distance like 100m, 4*4 MIMO antenna will provide good result.

So, we can have fixed and assure that, 4*4 MIMO antenna is showing clearly good result both for LOS and NLOS environment and both for omnidirectional and directional antenna.

4.3 AoA, AoD and PDP for 4*4 MIMO using different condition

The simulation of the selected model with different choice of parameters is carried out in this section. It should be noted that statistical channel modeling is focused on extracting models form the measured azimuth and elevation power spectrum using 3-D ray-tracing predictions and generating the required data when measurements are not available [113]. For the simulation, assumptions were made for both channel and antenna properties, which can be discussed in previous section.

To simulate a NLOS and LOS environment within the Dhaka metropolitan and surrounding areas, channel parameters were generated to match the average environmental variables. For example, the average barometric pressure in the Dhaka area is 1013 mbar, the average temperature is 20◦C, and average humidity is set to 65%. Combined with the channel parameters for 5G, the frequencies simulated were 28 GHz with an RF bandwidth of 800 MHz. For an average user, the transmitter to receiver separation were set to 100m, 300m, 500m with an (ideal) co-polarization reception angle. The antenna parameters used were set to standard values so that simulations remained constant and independent of antennas. The TX and RX array types were set to URA for higher throughput, in accordance with [114]. Antenna spacing was set to 0.5λ so that there was no chance for a receiving party to be out of range and the azimuth and elevation were set at 10◦ so that both azimuth and elevation beams could be used.

4.3.1 AOA and AOD Lobe Power Spectrum for NLOS environment

The AOA and AOD lobe power spectra reveal that between the 28 GHz simulations, we see a similar power level. The multipath power delays were seen to be a function of the azimuth angle for both TX and RX. The received power is plotted into polar plots for both the 28 GHz frequencies bands as shown in Figures 4.3.1.1, 4.3.1.2, 4.3.1.3 respectively.

Each ray represents the peak of a lobe3, where each lobe represents a possible propagation route. AOA and AOD can be defined as $\bar{\theta}$ which represents a power-weighted mean pointing angle (angle of direction). $\bar{\theta}$ can be used on each lobe to identify a single direction of energy arrival/departure calculated by,

$$\bar{\theta} = \frac{\sum_k P(\theta_k)\theta_k}{\sum_k P(\theta_k)} \qquad 4.3.1.1$$

Where k is the index of the pointing angle, in degrees, within a lobe and $P(\theta_k)$ is the received power at θ_k. Being that the results and values for both sets of data are randomly generated for differing distances, it is possible for a scenario to be precisely simulated using the 3-D SSCM. The mean value for a set of AOA/AOD rays, i.e. lobes, if measured or simulated in/for a surrounding area should return a uniform distribution between 0 to 360 degrees. As shown by Figures 4.3.1.1, 4.3.1.2, 4.3.1.3, the AOA/AOD lobe power spectra appear similar and closely related. The similarities in power spectra can be attributed to the transmitted power which is set to 30 dBm for all cases, and is not dependent on the frequency of transmission.

A. In 20^0 Celsius temperature with 110 mm/hr. rain rate in 300m T-R separation distance

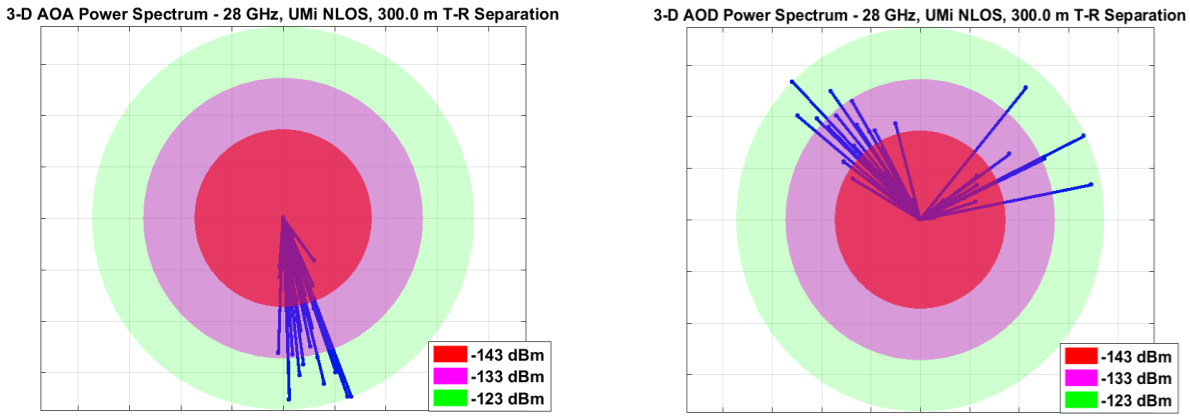

Fig. 4.3.1..1. AoD and AoA power spectrum for 28 GHz in 20^0 Celsius

B. In 15^0 Celsius temperature without rain rate in 300m T-R separation distance

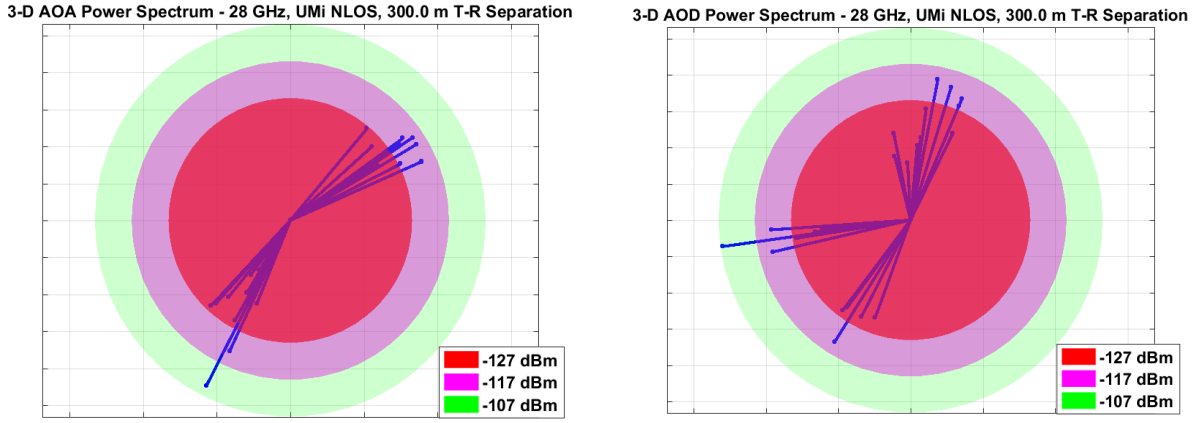

Fig. 4.3.1..2. AoD and AoA power spectrum for 28 GHz in 15^0 Celsius

C. In 30^0 Celsius temperature without rain rate in 500m T-R separation distance

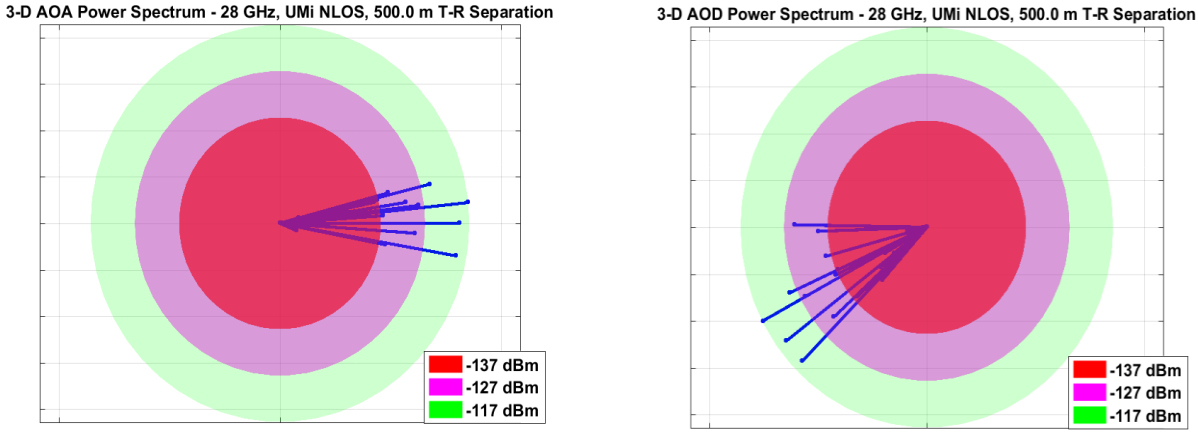

Fig. 4.3.1..3. AoD and AoA power spectrum for 28 GHz in 15^0 Celsius

4.3.2 AOA and AOD Lobe Power Spectrum for LOS environment

A. In 30^0 Celsius temperature without rain rate in 500m T-R separation distance

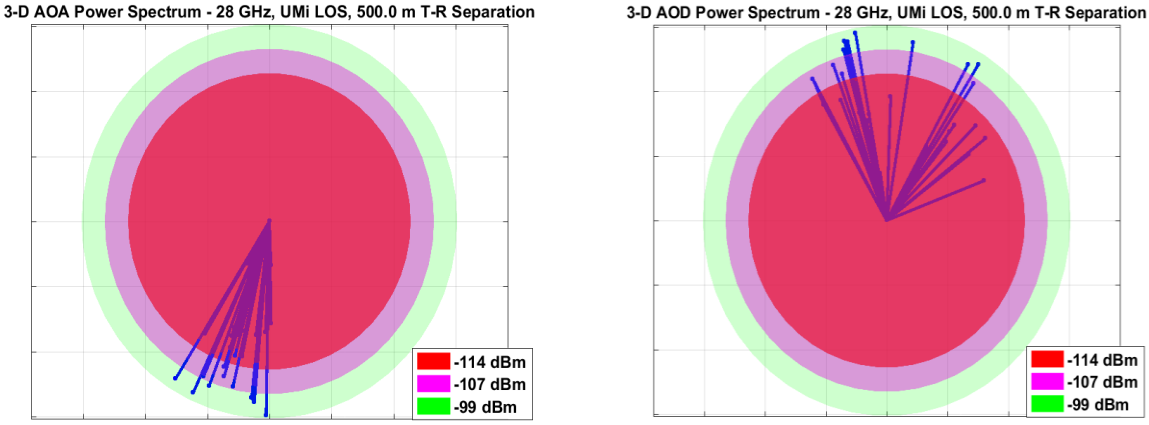

Fig. 4.3.2.1. AoD and AoA Power Spectrum for 28 GHz 30^0 Celsius

B. In 15^0 Celsius temperature without rain rate in 100m T-R separation distance

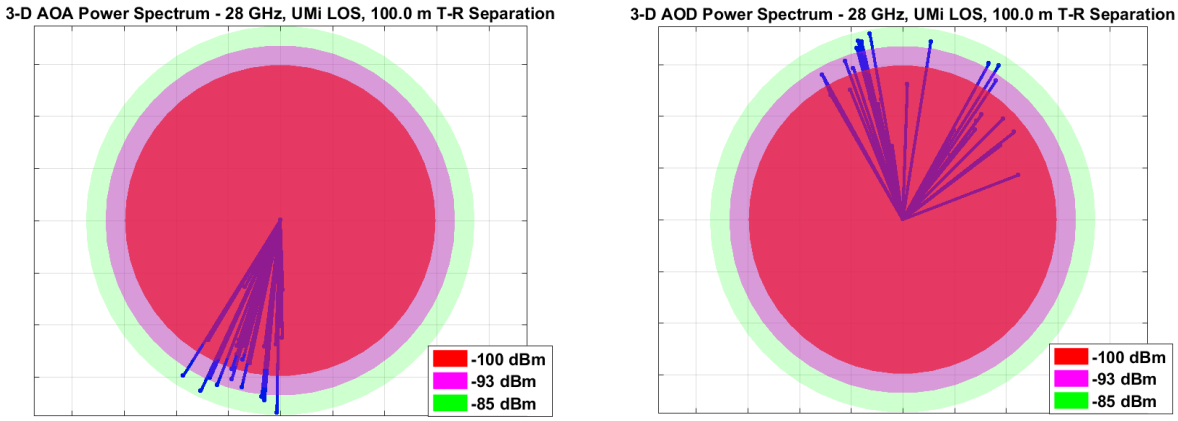

Fig. 4.3.2.2. AoD and AoA Power Spectrum for 28 GHz 15^0 Celsius

C. In 20^0 Celsius temperature with 100mm/hr. rain rate in 100m T-R separation distance

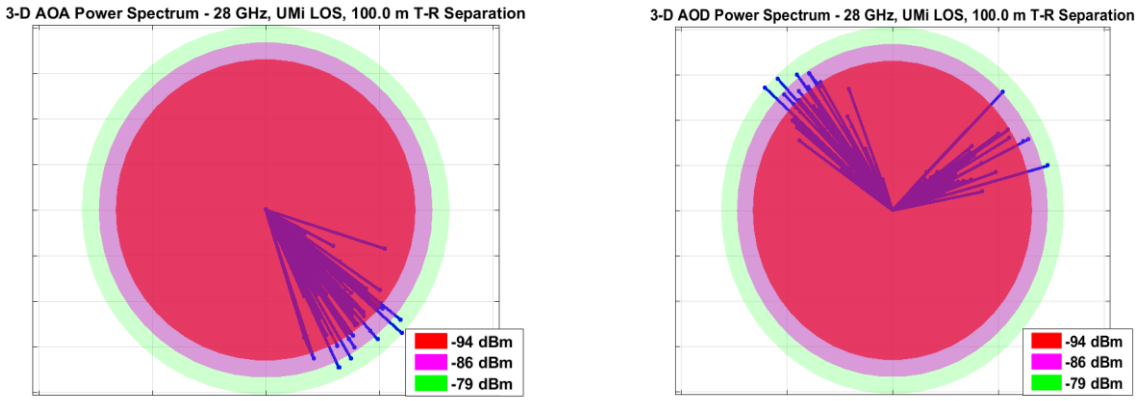

Fig. 4.3.2.3. AoD and AoA Power Spectrum for 28 GHz 30^0 Celsius

Both for NLOS and LOS environment AOA and AOD can be represents a power-weighted mean pointing angle (angle of direction). It can be used on each lobe to identify a single direction of energy arrival/departure. The mean value for a set of AOA/AOD rays, i.e. lobes, if measured or simulated in/for a surrounding area should return a uniform distribution between 0 to 360 degrees. As shown by 4.3.2.1, 4.3.2.2, 4.3.2.3 respectively, the AOA/AOD lobe power spectra appear similar and closely related. The similarities in power spectra can be attributed to the transmitted power which is set to 30 dBm for all cases, and is not dependent on the frequency of transmission.

4.3.3 Omnidirectional and directional power delay profile for 28 GHz NLOS and LOS at 20^0 temperature

In order to fully understand the channel, the propagation of the channel needs to be examined. Most usually, the propagation is described by the superposition of multiple traveling waves, where each impinging wave at the receiver is described by its path amplitude (voltage), delay, AOD, and AOA. From these components, a double-directional, i.e. omnidirectional, time-invariant channel impulse response (CIR) can be calculated by,

$$h_{omni}(t,\bar{\theta},\bar{\phi}) = \sum_{k=1}^{N} a_k e^{j\theta_k}\,\delta(t-\tau_k).\delta(\bar{\theta}-\bar{\theta}_k).\delta(\bar{\phi}-\bar{\phi}_k) \qquad 4.3.3.1$$

Where a_k, θ_k, and τ_k are amplitude, phase, and propagation delay, respectively, of the *kth* multipath component, $\bar{\theta}_k$ and $\bar{\phi}_k$. N represents the total number of resolvable path components, and $\delta()$ is the Dirac-delta function.

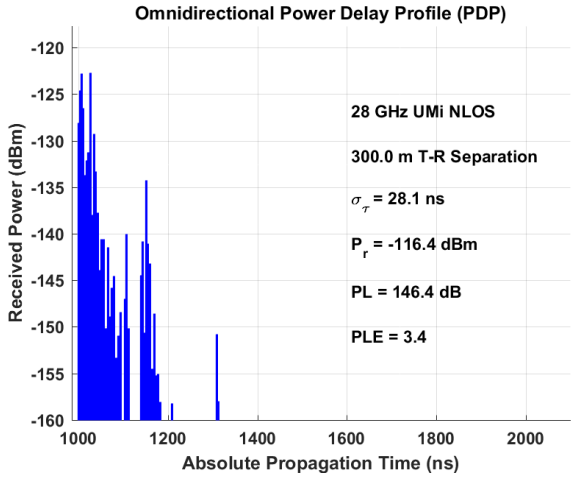

Fig. 4.3.3.1. Omnidirectional PDP for 28 GHz NLOS environment

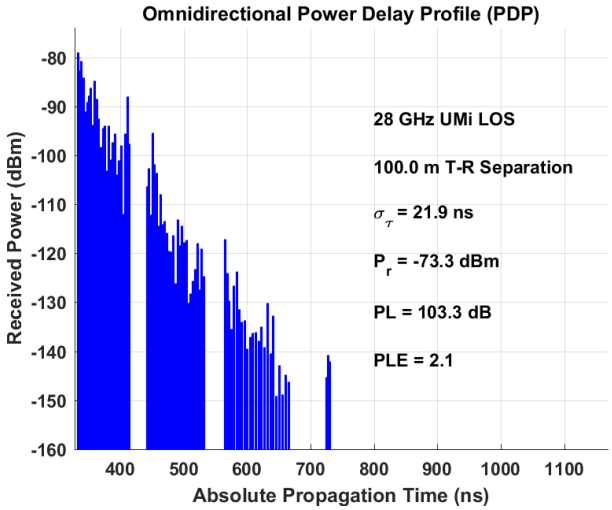

Fig. 4.3.3.2. Omnidirectional PDP for 28 GHz LOS environment

The 28 GHz bands proved to be similar in their propagation delays due to their relatively similar separation distances. As separation distances were increased in simulation, the absolute propagation time also increased. The slight differences in attenuation can be noted between the two separation distance in LOS and NLOS environment, and it is suspected

that, according to [115], a shadowing factor may have come into play which indicated more variability in shadowing at higher mmWave frequencies. The increased shadowing effect can be attributed to increased diffuse scattering, diffraction loss, and weaker reflections.

4.3.4 Directional and directional power delay profile for 28 GHz NLOS and LOS at 20^0

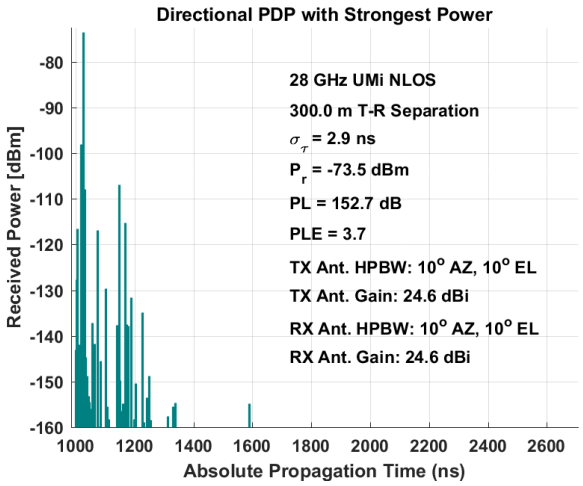

Fig. 4.3.4.1. Directional PDP for 28 GHz NLOS environment

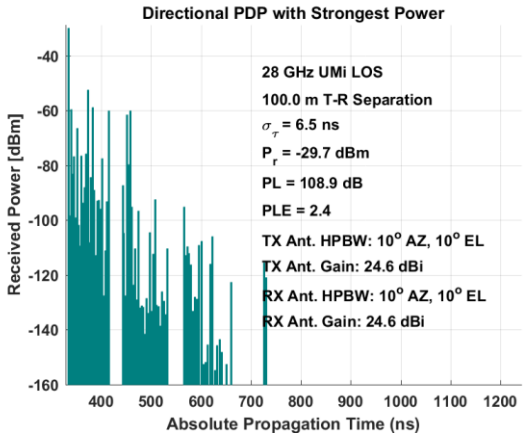

Fig. 4.3.4.2. Directional PDP for 28 GHz LOS environment

Directional PDP with strongest power in 28 GHz LOS and NLOS is presented in Figures 4.3.4.1 and 4.3.4.2. It shows that in LOS, the received power of PDP goes down after about 650 ns, whereas in NLOS, it goes down after about 1620 ns.

4.3.5 Path Loss

Path loss may occur due to various phenomena like free space path loss, reflection, diffraction, fading, shadowing, etc. There are a large number of theoretical analysis on path loss exponent estimation, without considering the practical measurements and environmental conditions.

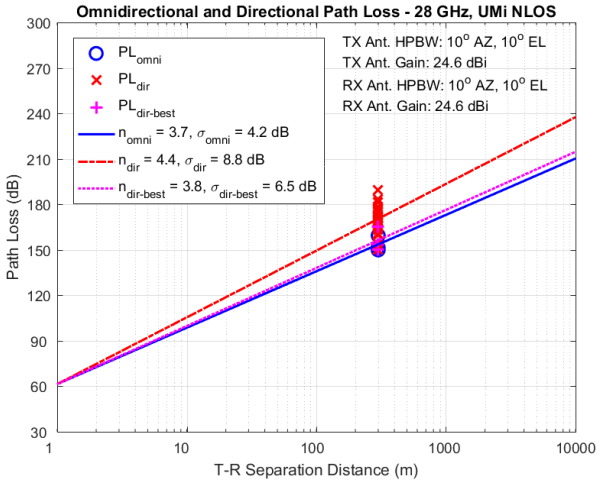

Fig. 4.3.5.1. Omnidirectional and directional path loss for 28 GHz NLOS

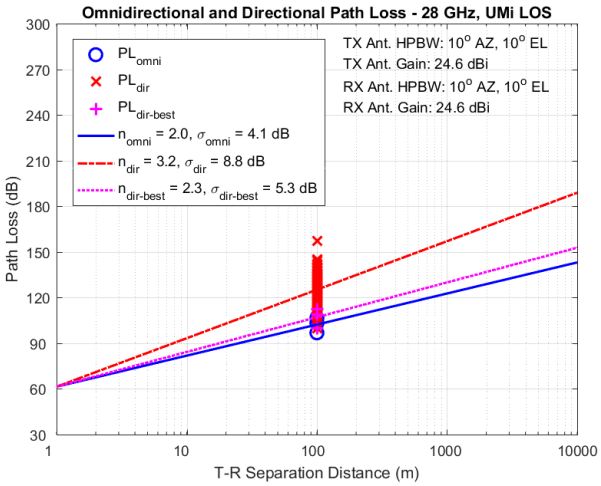

Fig. 4.3.5.2. Omnidirectional and directional path loss for 28 GHz LOS

The scatter plot shows the omnidirectional and directional path loss values generated for the 28 GHz UMi LOS and NLOS scenarios, with a T-R distance of about 300m for NOS,

and about 100m for LOS. The path-lost scattered between 90-160 dB for both NLOS and LOS.

It also shows fitted path loss exponent and shadow fading standard deviation, best direction from which strong signal is received. Directional path loss and directional path loss exponent are higher this is because directional channel is more lossy when compared to omnidirectional channel. This is because of the directional antenna filters out MPCs and receives few MPCs from a specific direction. Antenna elevation and azimuth HPBWs are set to 10° and 15° respectively at both transmitter and receiver. The results for PLE and shadow fading are in agreement with measured results in [119].

Chapter 5

Conclusion

In this thesis channel modelling of 5G mmWave cellular communication for urban microcell is simulated in LOS and NLOS condition at operating frequency of 28 GHz with multiple antenna elements at transmitter and receiver. Different parameters affecting the channel has been considered in simulation using NYUSIM software developed at NYU Wireless. Channel impulse response is generated for different simulation runs at different transmitter and receiver separations. Channel parameters like AoA/AoD power spectra, directional power delay profile, omnidirectional power delay profile at different antenna elements are recorded. Scatter plot of path loss as a function of distance for omnidirectional, directional and best direction is also produced with different statistical parameters like path loss, path loss exponent and standard deviation.

Also this thesis describes about the proper selection of antenna element for MIMO in 5G cellular mobile communication in 28 GHz frequency. This thesis also describes about the communication in NLOS and LOS environment. And also after that, the path loss and time dispersion estimated for 5G channels at 28 GHz frequency for LOS and NLOS environments also will be discussed on based on different parameter. A comparison study of LOS and NLOS performance in the 28 GHz band for Millimeter-Wave wireless networks has been discussed, including the performance for time delay, received power, azimuth AoD, Elevation AoD, Azimuth AoA, Elevation AoA, path-lost and RMS delay in LOS and NLOS environments. The time delay in LOS is greatly fluctuative whereas time delay in NLOS is more stable.

References

[1] F. Boccardi et al., “Five disruptive technology directions for 5G,” IEEE Communications Magazine, vol. 52, pp. 74–80, Feb. 2014.

[2] T. S. Rappaport, S. Sun, R. Mayzus, H. Zhao, Y. Azar, K. Wang, G. N. Wong, J. K. Schulz, M. Samimi, and F. Gutierrez, “Millimeter wave mobile communications for 5G cellular: It will work!” IEEE Access, vol. 1, pp. 335– 349, May 2013.

[3] Federal Communications Commission, “Spectrum frontiers rules identify,” Jul. 2016.

[4] S. Rangan, T. S. Rappaport, and E. Erkip, “Millimeter-wave cellular wireless networks: potentials & challenges,” in IEEE Proceedings, vol. 102, Mar. 2014.

[5] Cisco, “Cisco visual network index: Global mobile traffic forecast update,” Tech. Rep. 20162021 white paper, Mar. 2017.

[6] M. Shafi, A. F. Molisch, P. J. Smith, T. Haustein, P. Zhu, P. D. Silva, F. Tufvesson, A. Benjebbour, and G. Wunder, “5G: A tutorial overview of standards, trials, challenges, deployment, and practice,” IEEE Journal on Selected Areas in Communications, vol. 35, pp. 1201–1221, Jun. 2017.

[7] G. P. Fettweis, “The tactile internet: Applications and challenges,” IEEE Vehicular Technology Magazine, vol. 9, pp. 64–70, Mar. 2014.

[8] J. G. Andrews, S. Buzzi, W. Choi, S. V. Hanly, A. Lozano, A. C. K. Soong, and J. C. Zhang, “What will 5G be?,” IEEE Journal on Selected Areas in Communications, vol. 32, pp. 1065–1082, Jun. 2014.

[9] C. X. Wang, F. Haider, X. Gao, X. H. You, Y. Yang, D. Yuan, H. M. Aggoune, H. Haas, S. Fletcher, and E. Hepsaydir, “Cellular architecture and key technologies for 5G wireless communication networks,” IEEE Communications Magazine, vol. 52, pp. 122–130, Feb. 2014.

[10] X. Ge, H. Cheng, M. Guizani, and T. Han, “5G wireless backhaul networks: challenges and research advances,” IEEE Network, vol. 28, pp. 6–11, Nov. 2014.

[11] S. Hur, T. Kim, D. J. Love, J. V. Krogmeier, T. A. Thomas, and A. Ghosh, “Millimeter wave beamforming for wireless backhaul and access in small cell networks,” IEEE Transactions on Communications, vol. 61, pp. 4391–4403, Oct. 2013.

[12] M. Rumney, “Testing 5G: Time to throw away the cables,” Microwave Journal, Nov. 2016.

[13] T. L. Marzetta, “Noncooperative cellular wireless with unlimited numbers of base station antennas,” IEEE Transactions on Wireless Communications, vol. 9, pp. 3590–3600, Nov. 2010.

[14] F. Rusek, D. Persson, B. K. Lau, E. G. Larsson, T. L. Marzetta, O. Edfors, and F. Tufvesson, "Scaling up MIMO: Opportunities and challenges with 279 very large arrays," IEEE Signal Processing Magazine, vol. 30, pp. 40–60, Jan. 2013.

[15] E. G. Larsson, O. Edfors, F. Tufvesson, and T. L. Marzetta, "Massive MIMO for next generation wireless systems," IEEE Communications Magazine, vol. 52, pp. 186–195, Feb. 2014.

[16] L. Lu, G. Y. Li, A. L. Swindlehurst, A. Ashikhmin, and R. Zhang, "An overview of massive MIMO: Benefits and challenges," IEEE Journal of Selected Topics in Signal Processing, vol. 8, pp. 742–758, Oct. 2014.

[17] T. L. Marzetta, "Massive MIMO: An introduction," Bell Labs Technical Journal, vol. 20, pp. 11–22, 2015.

[18] E. Bjrnson, E. G. Larsson, and T. L. Marzetta, "Massive MIMO: ten myths and one critical question," IEEE Communications Magazine, vol. 54, pp. 114– 123, Feb. 2016.

[19] V. Jungnickel, K. Manolakis, W. Zirwas, B. Panzner, V. Braun, M. Lossow, M. Sternad, R. Apelfrojd, and T. Svensson, "The role of small cells, coordinated multipoint, and massive MIMO in 5G," IEEE Communications Magazine, vol. 52, pp. 44–51, May 2014.

[20] Federal Communications Commission, "Spectrum Frontiers Report and Order and Further Notice of Proposed Rulemaking: FCC16-89," July 2016.

[21] T. S. Rappaport, "Spectrum Frontiers: The New World of Millimeter-Wave Mobile Communication," Invited keynote presentation, The Federal Communications Commission (FCC) Headquarters, Mar. 10 2016.

[22] X. Cheng, B. Yu, L. Yang, J. Zhang, G. Liu, Y. Wu, and L. Wan, "Communicating in the real world: 3D MIMO," IEEE Wireless Communications, vol. 21, pp. 136–144, Aug. 2014.

[23] W. Roh, et al, "Millimeter-wave beamforming as an enabling technology for 5G cellular communications: theoretical feasibility and prototype results," IEEE Communications Magazine, vol. 52, pp. 106–113, Feb. 2014.

[24] S. Sun, T. S. Rappaport, R. W. Heath, A. Nix, and S. Rangan, "MIMO for millimeter-wave wireless communications: beamforming, spatial multiplexing, or both?," IEEE Communications Magazine, vol. 52, pp. 110–121, Dec. 2014.

[25] G. Xu, Y. Li, J. Yuan, R. Monroe, S. Rajagopal, S. Ramakrishna, Y. H. Nam, J. Y. Seol, J. Kim, M. M. U. Gul, A. Aziz, and J. Zhang, "Full dimension MIMO (FD-MIMO): Demonstrating commercial feasibility," IEEE Journal on Selected Areas in Communications, vol. 35, pp. 1876–1886, Aug. 2017.

[26] J. Zhang, Y. Zhang, Y. Yu, R. Xu, Q. Zheng, and P. Zhang, "3-D MIMO: How much does it meet our expectations observed from channel measurements?," IEEE Journal on Selected Areas in Communications, vol. 35, pp. 1887–1903, Aug. 2017.

[27] J. B. Andersen, T. S. Rappaport, and S. Yoshida, “Propagation measurements and models for wireless communications channels,” IEEE Communications Magazine, vol. 33, pp. 42–49, Jan. 1995.

[28] J. Medbo, P. Kyosti, K. Kusume, L. Raschkowski, K. Haneda, T. Jamsa, V. Nurmela, A. Roivainen, and J. Meinila, “Radio propagation modeling for 5G mobile and wireless communications,” IEEE Communications Magazine, vol. 54, pp. 144–151, Jun. 2016.

[29] T. S. Rappaport, Y. Xing, G. R. MacCartney, Jr., A. F. Molisch, E. Mellios, and J. Zhang, “Overview of millimeter wave communications for fifthgeneration (5G) wireless networks-with a focus on propagation models,” IEEE Transactions on Antennas and Propagation, Special Issue on 5G. to appear Dec. 2017.

[30] T. S. Rappaport, S. Sun, and M. Shafi, “Investigation and comparison of 3GPP and NYUSIM channel models for 5G wireless communications,” in 2017 IEEE 86th Vehicular Technology Conference (VTC-Fall), pp. 1–5, Sep. 2017.

[31] G.R. MacCartney, T. S. Rappaport, "A Flexible Millimeter-Wave Channel Sounder With Absolute Timing", Selected Areas in Communications IEEE Journal on, vol. 35, pp. 1402-1418, 2017.

[32] S. Sun, T. S. Rappaport, T. A. Thomas, A. Ghosh, H. C. Nguyen, I. Z. Kovcs, I. Rodriguez, O. Koymen, and A. Partyka, “Investigation of prediction accuracy, sensitivity, and parameter stability of large-scale propagation path loss models for 5G wireless communications,” IEEE Transactions on Vehicular Technology, vol. 65, pp. 2843–2860, May 2016.

[33] S. Sun, G. R. MacCartney, and T. S. Rappaport, “A novel millimeter-wave channel simulator and applications for 5G wireless communications,” in 2017 IEEE International Conference on Communications (ICC), May 2017.

[34] M. K. Samimi and T. S. Rappaport, “3-D millimeter-wave statistical channel model for 5G wireless system design,” IEEE Transactions on Microwave Theory and Techniques, vol. 64, pp. 2207–2225, Jul. 2016.

[35] T. S. Rappaport, G. R. MacCartney, Jr., M. K. Samimi, and S. Sun, “Wideband millimeter-wave propagation measurements and channel models for future wireless communication system design (Invited Paper),” IEEE Transactions on Communications, vol. 63, pp. 3029–3056, Sep. 2015.

[36] G. R. MacCartney and T. S. Rappaport, “Rural macrocell path loss models for millimeter wave wireless communications,” IEEE Journal on Selected Areas in Communications, vol. 35, pp. 1663–1677, Jul. 2017.

[37] G. R. MacCartney, T. S. Rappaport, S. Sun, and S. Deng, “Indoor office wideband millimeter-wave propagation measurements and channel models at 28 and 73 GHz for ultra-dense 5G wireless networks,” IEEE Access, vol. 3, pp. 2388–2424, Oct. 2015.

[38] M. K. Samimi and T. S. Rappaport, "Local multipath model parameters for generating 5G millimeter-wave 3GPP-like channel impulse response," in 2016 10th European Conference on Antennas and Propagation (EuCAP), pp. 1–5, Apr. 2016.

[39] G. R. MacCartney, Jr., S. Sun, T. S. Rappaport, Y. Xing, H. Yan, J. Koka, R. Wang, and D. Yu, "Millimeter wave wireless communications: New results for rural connectivity," in All Things Cellular16, in conjunction with ACM MobiCom, Oct. 2016.

[40] "Investigation of prediction accuracy, sensitivity, and parameter stability of large-scale propagation path loss models from 500 MHz to 100 GHz,"

[41] T. S. Rappaport, S. Sun, and M. Shafi, "5G channel model with improved accuracy and efficiency in mmWave bands," IEEE 5G Tech Focus, vol. 1, Mar. 2017.

[42] T. S. Rappaport, G. R. MacCartney, S. Sun, H. Yan, and S. Deng, "Smallscale, local area, and transitional millimeter wave propagation for 5G communications," IEEE Transactions on Antennas and Propagation, vol. 65, pp. 6474–6490, Dec. 2017.

[43] V. Fung, T. S. Rappaport, and B. Thoma, "Bit error simulation for pi/4 DQPSK mobile radio communications using two-ray and measurement-based impulse response models," IEEE Journal on Selected Areas in Communications, vol. 11, pp. 393–405, Apr. 1993.

[44] J. C. Liberti and T. S. Rappaport, "Analysis of CDMA cellular radio systems employing adaptive antennas in multipath environments," in IEEE 46th Vehicular Technology Conference, vol. 2, pp. 1076–1080, Apr. 1996.

[45] J. Lota, S. Sun, T. S. Rappaport, and A. Demosthenous, "5G uniform linear arrays with beamforming and spatial multiplexing at 28, 37, 64, and 71 GHz for outdoor urban communication: A two-level approach," IEEE Transactions on Vehicular Technology, vol. 66, pp. 9972–9985, Nov. 2017.

[46] 3GPP, "Study on channel model for frequencies from 0.5 to 100 GHz," TR 38.901 V14.3.0, 3rd Generation Partnership Project (3GPP), Dec. 2017.

[47] T. S. Rappaport, R. W. Heath, Jr., R. C. Daniels, and J. N. Murdock, Millimeter Wave Wireless Communications. Pearson/Prentice Hall 2015.

[48] S. Sun, T. S. Rappaport, T. A. Thomas, A. Ghosh, H. C. Nguyen, I. Z. Kovcs, I. Rodriguez, O. Koymen, and A. Partyka, "Investigation of prediction accuracy, sensitivity, and parameter stability of large-scale propagation path loss models for 5G wireless communications," IEEE Transactions on Vehicular Technology, vol. 65, pp. 2843–2860, May 2016.

[49] H. J. Liebe, G. A. Hu↵ord, and M. G. Cotton, "Propagation modeling of moist air and suspended water/ice particles at frequencies below 1000 GHz," AGARD Conference Proceedings 542, May 1993.

[50] J. J. A. Lempianen, J. K. Laiho-Ste↵ens, and A. F. Wacker, "Experimental results of cross polarization discrimination and signal correlation values for a polarization diversity scheme," in IEEE 47th Vehicular Technology Conference, vol. 3, pp. 1498–1502, May 1997.

[51] H. lin Xiao, S. Ouyang, and Z. ping Nie, "The cross polarization discrimination of MIMO antennas at mobile station," in International Conference on Communications, Circuits and Systems (ICCCAS), pp. 203–206, May 2008.

[52] T. S. Rappaport and S. Deng, "73 GHz wideband millimeter-wave foliage and ground reflection measurements and models," in 2015 IEEE International Conference on Communication Workshop (ICCW), pp. 1238–1243, June 2015.

[53] J. Meinil¨a, P. Ky¨osti, T. J¨ams¨a, and L. Hentil¨a, "Winner ii channel models," Radio Technologies and Concepts for IMT-Advanced, pp. 39–92, 2009.

[54] T. S. Rappaport and R. A. Brickhouse, "A simulation of cellular system growth and its e↵ect on urban in-building parasitic frequency reuse," IEEE Transactions on Vehicular Technology, vol. 48, pp. 286–294, Jan. 1999.

[55] T. Bai, A. Alkhateeb, and R. W. Heath, "Coverage and capacity of millimeterwave cellular networks," IEEE Communications Magazine, vol. 52, pp. 70–77, Sep. 2014.

[56] A. F. Molisch, Wireless communications, vol. 34. John Wiley & Sons, 2012.

[57] E. K. Smith, "Centimeter and millimeter wave attenuation and brightness temperature due to atmospheric oxygen and water vapor," Radio Science, vol. 17, no. 06, pp. 1455–1464, 1982.

[58] H. J. Liebe, "An updated model for millimeter wave propagation in moist air," Radio Science, vol. 20, no. 5, pp. 1069–1089, 1985.

[59] ITU-R, "Specific attenuation model for rain for use in prediction methods, propagation in non-ionized media," Tech. Rep. P.838-3, 2005.

[60] ITU-R, "Attenuation by atmospheric gases," Tech. Rep. P.676-8, 2009.

[61] H. Zhao, R. Mayzus, S. Sun, M. Samimi, J. K. Schulz, Y. Azar, K. Wang, G. N. Wong, F. Gutierrez, and T. S. Rappaport, "28 GHz millimeter wave cellular communication measurements for reflection and penetration loss in and around buildings in new york city," in 2013 IEEE International Conference on Communications (ICC), pp. 5163–5167, Jun. 2013.

[62] X. Chen, L. Tian, P. Tang, and J. Zhang, "Modelling of human body shadowing based on 28 ghz indoor measurement results," in Vehicular Technology Conference (VTC-Fall), 2016 IEEE 84th, pp. 1–5, IEEE, 2016.

[63] M. R. Akdeniz, Y. Liu, M. K. Samimi, S. Sun, S. Rangan, T. S. Rappaport, and E. Erkip, "Millimeter wave channel modeling and cellular capacity evaluation," IEEE Journal on Selected Areas in Communications, vol. 32, pp. 1164–1179, Jun. 2014.

[64] M. R. Akdeniz, Y. Liu, M. K. Samimi, S. Sun, S. Rangan, T. S. Rappaport, and E. Erkip, "Millimeter wave channel modeling and cellular capacity evaluation," IEEE Journal on Selected Areas in Communications, vol. 32, pp. 1164–1179, Jun. 2014.

[65] S. Han, I. Chih-Lin, Z. Xu, and C. Rowell, "Large-scale antenna systems with hybrid analog and digital beamforming for millimeter wave 5G," IEEE Communications Magazine, vol. 53, pp. 186–194, Jan. 2015.

[66] Y. Zeng and R. Zhang, "Millimeter wave MIMO with lens antenna array: A new path division multiplexing paradigm," IEEE Transactions on Communications, vol. 64, pp. 1557–1571, Apr. 2016.

[67] Y. Wang, Z. Shi, L. Huang, Z. Yu, and C. Cao, "An extension of spatial channel model with spatial consistency," in Vehicular Technology Conference (VTC-Fall), 2016 IEEE 84th, pp. 1–5, IEEE, 2016.

[68] Y. Tan, C. X. Wang, J. Nielsen, and G. F. Pedersen, "Comparison of stationarity regions for wireless channels from 2 GHz to 30 GHz," in 2017 13th International Wireless Communications and Mobile Computing Conference (IWCMC), pp. 647–652, Jun. 2017.

[69] ITU-R, "M. 2135: guidelines for evaluation of radio interface technologies for imt-advanced," 2008.

[70] T. S. Rappaport, R. W. Heath, Jr., R. C. Daniels, and J. N. Murdock, Millimeter Wave Wireless Communications. Pearson/Prentice Hall, 2015.

[71] F. Gutierrez, S. Agarwal, K. Parrish, and T. S. Rappaport, "On-chip integrated antenna structures in CMOS for 60 GHz WPAN systems," IEEE Journal on Selected Areas in Communications, vol. 27, no. 8, pp. 1367– 1378, October 2009.

[72] Z. Pi and F. Khan, "An introduction to millimeter-wave mobile broadband systems," IEEE Communications Magazine, vol. 49, no. 6, pp. 101–107, June 2011.

[73] Z. Pi and F. Khan, "An introduction to millimeter-wave mobile broadband systems," IEEE Communications Magazine, vol. 49, no. 6, pp. 101–107, June 2011.

[74] A. Osseiran, F. Boccardi, V. Braun, K. Kusume, P. Marsch, M. Maternia, O. Queseth, M. Schellmann, H. Schotten, H. Taoka, H. Tullberg, M. A. Uusitalo, B. Timus, and M. Fallgren, "Scenarios for 5G mobile and wireless communications: The vision of the METIS project," vol. 52, no. 5, pp. 26–35, May 2014.

[75] A. Osseiran, F. Boccardi, V. Braun, K. Kusume, P. Marsch, M. Maternia, O. Queseth, M. Schellmann, H. Schotten, H. Taoka et al., "Scenarios for 5g mobile and wireless communications: the vision of the metis project," IEEE Communications Magazine, vol. 52, no. 5, pp. 26–35, 2014.

[76] M. R. Palattella, M. Dohler, A. Grieco, G. Rizzo, J. Torsner, T. Engel, and L. Ladid, "Internet of things in the 5g era: Enablers, architecture, and business models," IEEE Journal on Selected Areas in Communications, vol. 34, no. 3, pp. 510–527, 2016.

[77] C.-X. Wang, F. Haider, X. Gao, X.-H. You, Y. Yang, D. Yuan, H. Aggoune, H. Haas, S. Fletcher, and E. Hepsaydir, "Cellular architecture and key technologies for 5g wireless communication networks," IEEE Communications Magazine, vol. 52, no. 2, pp. 122–130, 2014.

[78] F. Rusek, D. Persson, B. K. Lau, E. G. Larsson, T. L. Marzetta, O. Edfors, and F. Tufvesson, "Scaling up mimo: Opportunities and challenges with very large arrays," IEEE Signal Processing Magazine, vol. 30, no. 1, pp. 40–60, 2013.

[79] G.R. MacCartney, T. S. Rappaport, "A Flexible Millimeter-Wave Channel Sounder With Absolute Timing", Selected Areas in Communications IEEE Journal on, vol. 35, pp. 1402-1418, 2017.

[80] J. Lota, S. Sun, T. S. Rappaport, A. Demosthenous, "5G Uniform Linear Arrays With Beamforming and Spatial Multiplexing at 28 37 64 and 71 GHz for Outdoor Urban Communication: A Two-Level Approach", Vehicular Technology IEEE Transactions on, vol. 66, pp. 9972-9985, 2017.

[81] "Channel modeling – an Introduction" Available on: https://www.gaussianwaves.com/2013/07/channel-modeling-an-introduction/

[82] T. S. Rappaport, S. Sun, and M. Shafi, "5G channel model with improved accuracy and efficiency in mmwave bands," *IEEE 5G Tech Focus*, vol. 1, no. 1, Mar. 2017.

[83] M. M. Lodro, N. Majeed, A. A. Khuwaja, A. H. Sodhro and S. Greedy, "Statistical channel modelling of 5G mmWave MIMO wireless communication," *2018 International Conference on Computing, Mathematics and Engineering Technologies (iCoMET)*, Sukkur, 2018, pp. 1-5.

[84] "5G Channel Models: Requirements and Deployment Scenarios", Available on: http://www.techplayon.com/5g-channel-models-requirements-deployment-scenarios/

[85] "5G Channel Modelling for Different Environments" Available on: www.5gworkshops.com/5G_Channel_Model_for_bands_up_to100_GHz(2015-12-6).pdf 5G Channel modeling for different environment

[86] J. I. Smith, "A computer generated multipath fading simulation for mobile radio," *IEEE Transactions on Vehicular Technology*, vol. 24, no. 3, pp. 39–40, Aug 1975.

[87] R. H. Clarke, "A statistical theory of mobile-radio reception," *The Bell System Technical Journal*, vol. 47, no. 6, pp. 957–1000, July 1968.

[88] S. Jaeckel *et al.*, "QuaDRiGa: A 3-D multi-cell channel model with time evolution for enabling virtual field trials," *IEEE Transactions on Antennas and Propagation*, vol. 62, no. 6, pp. 3242–3256, June 2014.

[89] Y. Yu *et al.*, "Propagation model and channel simulator under indoor stair environment for machine-to-machine applications," in *2015 Asia- Pacific Microwave Conference*, vol. 2, Dec. 2015, pp. 1–3.

[90] T. S. Rappaport *et al.*, "Statistical channel impulse response models for factory and open plan building radio communicate system design," *IEEE Transactions on Communications*, vol. 39, no. 5, pp. 794–807, May 1991.

[91] Wireless Valley Communications, Inc., *SMRCIM Plus 4.0 (Simulation of Mobile Radio Channel Impulse Response Models) Users Manual*, Aug. 1999.

[92] V. K. Rajendran *et al.*, "Concepts and implementation of a semantic web archiving and simulation system for rf propagation measurements," in *2011 IEEE Vehicular Technology Conference (VTC Fall)*, Sept 2011, pp. 1–5.

[93] V. Fung *et al.*, "Bit error simulation for pi/4 DQPSK mobile radio communications using two-ray and measurement-based impulse response models," *IEEE Journal on Selected Areas in Communications*, vol. 11, no. 3, pp. 393–405, Apr. 1993.

[94] T. S. Rappaport et al., "Millimeter wave mobile communications for 5G cellular: It will work!" IEEE Access, vol. 1, pp. 335–349, May 2013.

[95] T. S. Rappaport et al., "Wideband millimeter-wave propagation measurements and channel models for future wireless communication system design (Invited Paper)," IEEE Transactions on Communications, vol. 63, no. 9, pp. 3029– 3056, Sep. 2015.

[96] M. K. Samimi and T. S. Rappaport, "3-D millimeter-wave statistical channel model for 5G wireless system design," IEEE Transactions on Microwave Theory and Techniques, vol. 64, no. 7, pp. 2207–2225, Jul. 2016.

[97] ——, "Local multipath model parameters for generating 5G millimeter-wave 3GPP-like channel impulse response," in 2016 10th European Conference on Antennas and Propagation (EuCAP), Apr. 2016, pp. 1–5.

[98] S. Sun et al., "A novel millimeter-wave channel simulator and applications for 5G wireless communications," in 2017 IEEE International Conference on Communications (ICC), May 2017.

[99] "Investigation of prediction accuracy, sensitivity, and parameter stability of large-scale propagation path loss models for 5G wireless communications," IEEE Transactions on Vehicular Technology, vol. 65, no. 5, pp. 2843–2860, May 2016.

[100] T. A. Thomas et al., "A prediction study of path loss models from 2-73.5 GHz in an urban-macro environment," in 2016 IEEE 83rd Vehicular Technology Conference (VTC Spring), May 2016, pp. 1–5.

[101] G. R. MacCartney et al., "Indoor office wideband millimeter-wave propagation measurements and channel models at 28 and 73 GHz for ultra-dense 5G wireless networks," IEEE Access, vol. 3, pp. 2388–2424, Oct. 2015.

[102] G. R. MacCartney and T. S. Rappaport, "Rural macrocell path loss models for millimeter wave wireless communications," IEEE Journal on Selected Areas in Communications, vol. 35, no. 7, pp. 1663–1677, Jul. 2017.

[103] T. S. Rappaport *et al.*, "Millimeter wave mobile communications for 5G cellular: It will work!" *IEEE Access*, vol. 1, pp. 335–349, 2013.

[104] "Wideband millimeter-wave propagation measurements and channel models for future wireless communication system design (Invited Paper)," *IEEE Transactions on Communications*, vol. 63, no. 9, pp. 3029–3056, Sep. 2015.

[105] M. K. Samimi and T. S. Rappaport, "3-D millimeter-wave statistical channel model for 5G wireless system design," *IEEE Transactions on Microwave Theory and Techniques*, vol. 64, no. 7, pp. 2207–2225, July 2016

[106] "Local multipath model parameters for generating 5G millimeter wave 3GPP-like channel impulse response," *the 10th European Conference on Antennas and Propagation (EuCAP 2016)*, April 2016.

[107] S. Sun *et al.*, "Investigation of prediction accuracy, sensitivity, and parameter stability of large-scale propagation path loss models for 5G wireless communications," *IEEE Transactions on Vehicular Technology*, vol. 65, no. 5, pp. 2843–2860, May 2016.

[108] "Synthesizing omnidirectional antenna patterns, received power and path loss from directional antennas for 5G millimeter-wave communications," in *2015 IEEE Global Communications Conference (GLOBECOM)*, Dec. 2015, pp. 1–7.

[109] G. R. MacCartney, Jr. *et al.*, "Indoor office wideband millimeter-wave propagation measurements and channel models at 28 and 73 GHz for ultra-dense 5G wireless networks," *IEEE Access*, vol. 3, pp. 2388–2424, Oct. 2015.

[110] "Millimeter wave wireless communications: New results for rural connectivity," in *All Things Cellular16, in conjunction with ACM MobiCom*, Oct. 2016.

[111] G. R. MacCartney, Jr. and T. S. Rappaport, "Study on 3GPP rural macrocell path loss models for millimeter wave wireless communications," in *2017 IEEE International Conference on Communications (ICC)*, May 2017, pp. 1–7.

[112] R. B. Ertel *et al.*, "Overview of spatial channel models for antenna array communication systems," *IEEE Personal Communications*, vol. 5, no. 1, pp. 10–22, Feb 1998.

[113] S. Sun *et al.*, "MIMO for millimeter-wave wireless communications: beamforming, spatial multiplexing, or both?" *IEEE Communications Magazine*, vol. 52, no. 12, pp. 110–121, Dec. 2014.

[114] N. Moraitis and P. Constantinou, "Indoor channel capacity evaluation utilizing ula and ura antennas in the millimeter wave band," in *Personal, Indoor and Mobile Radio Communications, 2007. PIMRC 2007. IEEE 18th International Symposium on*. IEEE, 2007, pp. 1–5.

[115] G. R. MacCartney, T. S. Rappaport, S. Sun, and S. Deng, "Indoor office wideband millimeter-wave propagation measurements and channel models at 28 and 73 ghz for ultra-dense 5g wireless networks," *IEEE Access*, vol. 3, pp. 2388–2424, 2015.

[116] J. Keignart, J. Pierrot, N. Daniele, A. Alvarez, M. Lobeira, J. Garcia, G. Valera, and R. Torres, “Ucan report on uwb basic transmission loss,” *Tech. Rep. IST-2001-32710 UCAN*, 2003.

[117] S. Piersanti, L. A. Annoni, and D. Cassioli, “Millimeter waves channel measurements and path loss models,” in *Communications (ICC), 2012 IEEE International Conference on*. IEEE, 2012, pp. 4552–4556.

[118] N. L. Johnson, S. Kotz, and N. Balakrishnan, *Discrete multivariate distributions*. Wiley New York, 1997, vol. 165.

[119] S. Sun, G. R. MacCartney, M. K. Samimi, and T. S. Rappaport, “Synthesizing omnidirectional received power and path loss from directional measurements at millimeter-wave frequencies,” in *2015 IEEE Global Telecommunications Conference (GLOBECOM 2015)*, 2015, pp. 3948– 3953.

[120] "Climate Information Management System", Climate.barcapps.gov.bd, 2018. [Online]. Available: http://climate.barcapps.gov.bd. [Accessed: 22- Apr- 2018].

[121] "timeanddate.com", Timeanddate.com, 2018. [Online]. Available: https://www.timeanddate.com/. [Accessed: 22- Apr- 2018].

[122] "Relative Humidity in Dhaka, Bangladesh", Dhaka.climatemps.com, 2018. [Online]. Available: http://www.dhaka.climatemps.com/humidity.php. [Accessed: 21- Jul- 2018].